



university of  
groningen

faculty of science  
and engineering

---

# Modelling and Simulation of a CMOS Synapse Implementing Two-phase Plasticity

---

*Author:*

Martin Alex NICHOLSON  
s4704088

*Supervisor:*

Dr. Erika COVI

*Second examiner :*

Prof. Elisabetta CHICCA

Bachelor's Thesis  
To fulfill the requirements for the degree of  
Bachelor of Science in Applied Physics  
at the University of Groningen

July 12, 2024

# Contents

	Page
<b>List of Figures</b>	<b>3</b>
<b>Abstract</b>	<b>5</b>
<b>Acknowledgements</b>	<b>6</b>
<b>1 Introduction</b>	<b>7</b>
<b>2 State of the Art</b>	<b>8</b>
2.1 Spiking neural networks: . . . . .	8
2.1.1 Introduction to SNNs . . . . .	8
2.1.2 SNN architecture: spiking neuron models . . . . .	9
2.2 Synaptic tagging and capture . . . . .	10
2.2.1 Calcium concentration . . . . .	11
2.2.2 Early-phase weight . . . . .	12
2.2.3 Late-phase weight . . . . .	13
2.3 Implementation of STC in the CMOS circuits . . . . .	15
2.3.1 Calculation of the calcium concentration in the CMOS circuits . . . . .	15
2.3.2 Calculation of the early-phase weight in the CMOS circuits . . . . .	16
<b>3 Results</b>	<b>18</b>
3.1 Summary of methods . . . . .	18
3.2 Reproduction of the synapse circuits in Python . . . . .	18
3.2.1 Testing of the synapse circuit-based script . . . . .	18
3.2.2 Comparison of the circuit-based script to literature . . . . .	20
3.3 Creation of an SNN to investigate the behaviour of the synapse circuitry at a network level . . . . .	22
3.3.1 Network architecture . . . . .	22
3.3.2 Training and testing . . . . .	23
<b>4 Discussion</b>	<b>28</b>
<b>5 Conclusion</b>	<b>32</b>
<b>Appendices</b>	<b>36</b>

## List of Figures

1	Overview of SNNs . . . . .	8
2	The LIF neuron . . . . .	10
3	An overview of STC . . . . .	11
4	STC: calcium concentration response . . . . .	12
5	STC: early-phase weight response . . . . .	13
6	STC: late-phase weight response . . . . .	14
7	Differential pair integrator circuit . . . . .	16
8	Early-phase circuitry block diagram . . . . .	17
9	Comparison of circuit-based script and differential equation script . . . . .	19
10	Early-phase weight change showing potentiation, depression and recovery . . . . .	20
11	Comparison of circuit-based script, differential equation script, circuit simulation and literature . . . . .	21
12	The encoding of a handwritten '3' as an MNIST sample. Figure extracted from [29].	22
13	Network architecture . . . . .	23
14	Synaptic weight response in various scenarios . . . . .	25
15	Heat map of synaptic weights - MNIST . . . . .	26
16	Overestimation of LPW in circuit simulation . . . . .	29
17	Influence of non-idealities on circuit behaviour . . . . .	30

## Glossary

**ANN** Artificial neural network.

**CMOS** Complementary metal-oxide-semiconductor.

**DC** Direct current.

**DPI** Differential pair integrator.

**EPW** Early-phase weight.

**GPU** Graphis processing unit.

**LIF** Leaky integrate-and-fire.

**LPW** Late-phase weight.

**MNIST** Modified National Institute of Standards and Technology.

**RAM** Random access memory.

**SNN** Spiking neural network.

**STC** Synaptic tagging and capture.

## Abstract

Spiking neural networks are promising candidates in the search for energy efficient neuromorphic systems. This work serves as a milestone in the development of in-silicon emulations of spiking neural networks by evaluating the behaviour of a CMOS synapse, implementing the multi-timescale learning rule synaptic tagging and capture, at a network level. Synaptic tagging and capture is a biologically plausible explanation of memory storage and recall in the mammalian neocortex that operates on two time scales: the early- and the late-phases of synaptic weight change. A set of CMOS circuits have been proposed, performing synaptic tagging and capture, which this thesis replicates in a Python environment. The validity of this Python replication is corroborated by comparisons of the circuit-based script to another Python script, which was written to solve the differential equations governing synaptic tagging and capture, and by comparisons to simulations of the CMOS circuits performed in Cadence Virtuoso. The circuit-based Python script is then incorporated in a virtual spiking neural network trained on the MNIST dataset, achieving an accuracy of 96% when testing is performed on the early-phase timescale, and 93% when performed on the late-phase timescale. This is used as evidence of the functionality of the proposed CMOS synapse on a network level.

## Acknowledgments

I would like to express my deepest gratitude to Dr. Erika Covi, and by extension CogniGron and the entire BICS group (chaired by Prof. Dr. Elisabetta Chicca), for providing me with the opportunity to carry out this work. I also thank Dr. Erika Covi for her unwavering support, feedback and input throughout this project, alongside Dr. Fernando M. Quintana for his invaluable insights into the field of computer science. My thanks also extend to Luca Fehlings, Paolo Gibertini, Bojian Zhang, Egidio Angelo Gallicchio and Pedro Francisco Ortiz Costa for their eagerness to help and the truly welcoming environment they provide.

Finally, I would like to offer special thanks to Jorge Navarro Quijada, who is responsible for the very basis on which this work stands, as he is the designer of the proposed CMOS synapse implementing two-phase plasticity.

# 1 Introduction

Neural networks have become an invaluable tool in resolving issues in natural language processing, computer vision and autonomous systems, even capable of outperforming the human brain at a variety of tasks [1, 2, 3, 4, 5, 6]. However, despite their many successes, neural networks are yet to approach the unparalleled efficiency of the human brain [7]. The brain consumes about 20 W of power [7], accumulating to about 18 000 kWh over the course of 100 years. This is a full order of magnitude lower than the estimated energy it took to train OpenAI’s GPT-3 language model [7], and although GPT-3 may outperform the brain in terms of knowledge, it certainly does not outperform it in terms of functionality. A potential approach to bridging this efficiency gap lies in the transition to more biologically plausible neural networks, which aim to connect the performance of artificial intelligence with the power efficiency of a biological system. Among the promising candidates for this transition are spiking neural networks (SNNs) [8], which will be the focus of this work.

SNNs aim to mimic the behaviour of the brain, making use of biologically plausible neuron and synapse models. Through doing so, SNNs exhibit the potential for increased efficiency relative to their predecessor, the artificial neural network (ANN) [9]. The primary strength of SNNs lies in their asynchronous, event-driven operation. They process information using spikes, for instance in the form of binary digital signals, and hence, neurons within the network only activate when necessary [10], reducing energy consumption [9]. This is in contrast to synchronous digital systems, including ANNs, that rely on periodic clock pulses and thus are continuously active [10].

This work investigates a potential path towards high efficiency SNNs, through the incorporation of the biologically inspired multi-timescale learning rule synaptic tagging and capture (STC) [11] in an SNN. STC is a biologically plausible explanation of how synaptic weights in the brain are updated, describing how memories are stored and recalled [11]. A set of complementary metal-oxide-semiconductor (CMOS) circuits have been proposed, implementing STC in circuitry. Such circuits would make it possible to construct physical neural networks performing this biologically plausible learning rule [12].

The aim of this work is to replicate these circuits in a Python environment and use this emulation to demonstrate their functionality at a network level. To achieve this, a complementary Python script was first developed to solve the differential equations governing STC, which was used in conjunction with circuit simulations to validate the Python replication of the circuitry. Subsequently, a virtual SNN was constructed incorporating the circuit-based Python replication to simulate the behavior of the circuits at the network level.

## 2 State of the Art

This work emulates in Python code the proposed CMOS circuits implementing the biologically inspired learning rule, STC, and then tests the Python code in an SNN. The following section provides an overview of SNNs, an explanation of STC, and finally an introduction as to how STC was implemented in the CMOS circuits.

### 2.1 Spiking neural networks:

#### 2.1.1 Introduction to SNNs

SNNs are a type of biologically inspired neural network, developed with the purpose of matching the performance of ANNs with the efficiency of the human brain. The biological equivalents of the components comprising an SNN are illustrated in Figure 1. Among the key differences between ANNs and SNNs is that the former operates using floating point numbers to transfer information between neurons, whereas the latter uses a more biologically plausible approach [13]. Biological neurons transmit information via action potentials. Action potentials are the rapid rise and fall of a neuron's membrane potential in response to its electrical and chemical inputs surpassing certain thresholds [14]. Owing to this rapidness, action potentials can be treated as discrete, binary spikes: an all-or-nothing event communicating the state of one neuron to its surrounding neurons via the synapses that connect them [7]. This allows the behaviour of a neuron to be described using binary arrays, with '1's representing a spike in discrete time, and '0's representing inactivity.

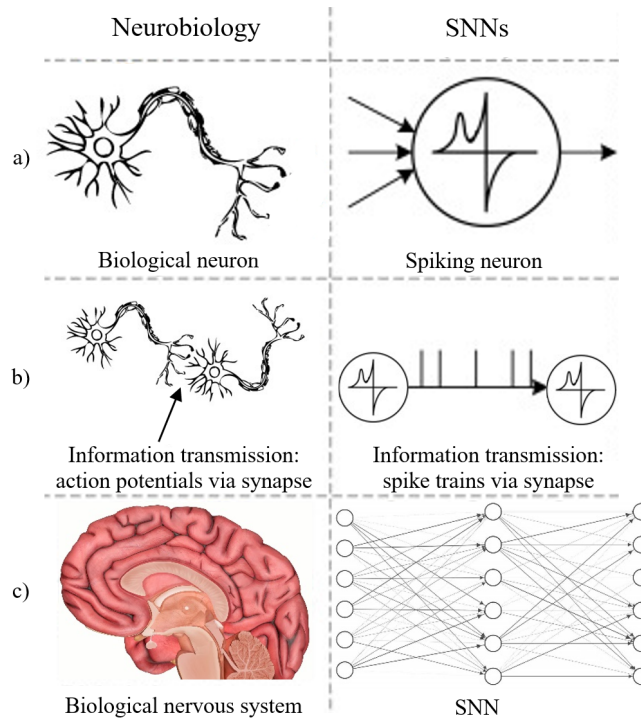


Figure 1: A comparison of the components of SNNs and their biological counterparts. (a) A biological neuron is modeled using a spiking neuron, as described in Section 2.1.2. (b) Information is transmitted by synapses. Biological synapses transmit action potentials, which are modeled as discrete spikes in SNNs. (c) SNNs aim to mimic the behaviour of the brain. Figure adapted from [15, 16, 17].



Since biological neurons spend the majority of their time inactive, the spiking activity of the biologically inspired neurons in SNNs tends to be limited [7]. As spiking activity is limited, the binary arrays describing neuron behaviours are sparse, meaning they contain far more zeroes than ones. This allows for data compression techniques such as run-length encoding to be incorporated into the SNNs, reducing their memory requirements, alongside their power consumption [7]. Hence, although ANNs still outperform their younger counterpart in certain areas, the improved energy and spatial efficiency of SNNs make them more suitable in edge computing applications, where power availability, space and access to a central cloud-based platform are limited. These types of applications were the initial motivation for the development of the CMOS circuits reproduced in this work [7].

### 2.1.2 SNN architecture: spiking neuron models

The leaky integrate-and-fire (LIF) neuron model was used in the creation of the SNN, chosen for its prevalence in neuromorphic computing and the balance it achieves between biological accuracy and computational efficiency [18]. Like biological neurons, LIF neurons are mostly inactive: they only spike once the membrane voltage of the neuron surpasses a certain threshold. The behaviour of the membrane voltage of a LIF neuron  $i$  is given by:

$$\tau_m \frac{d}{dt} V_i(t) = -V_i(t) + V_{rev} + \sum_j \sum_{t_j^k} w_{ji} \cdot \exp[-(t - t_j^k - t_{ax,delay})/\tau_{syn}] + R_m(I_{bg}(t) + I_{stim}(t)), \quad (1)$$

with membrane time constant  $\tau_m$ ; synaptic time constant  $\tau_{syn}$ ; reversal potential  $V_{rev}$ , which is the membrane potential at equilibrium; synaptic weights  $w_{ji}$  (with  $j$  being the index of presynaptic neurons and  $i$  the index of the neuron being described); presynaptic spike times  $t_j^k$ ; axon delay time  $t_{ax,delay}$ ; membrane resistance  $R_m$ ; background current  $I_{bg}(t)$ ; and stimulus current  $I_{stim}(t)$  [11, 19]. The neuron  $i$  spikes once  $V_i(t)$  surpasses the spiking threshold  $V_{th}$ , after which the neuron's membrane potential is set to  $V_{reset}$ . Following each spike, the potential remains at  $V_{reset}$  for the length of the refractory period  $t_{ref}$  [11, 19]. This behaviour is depicted in Figure 2.

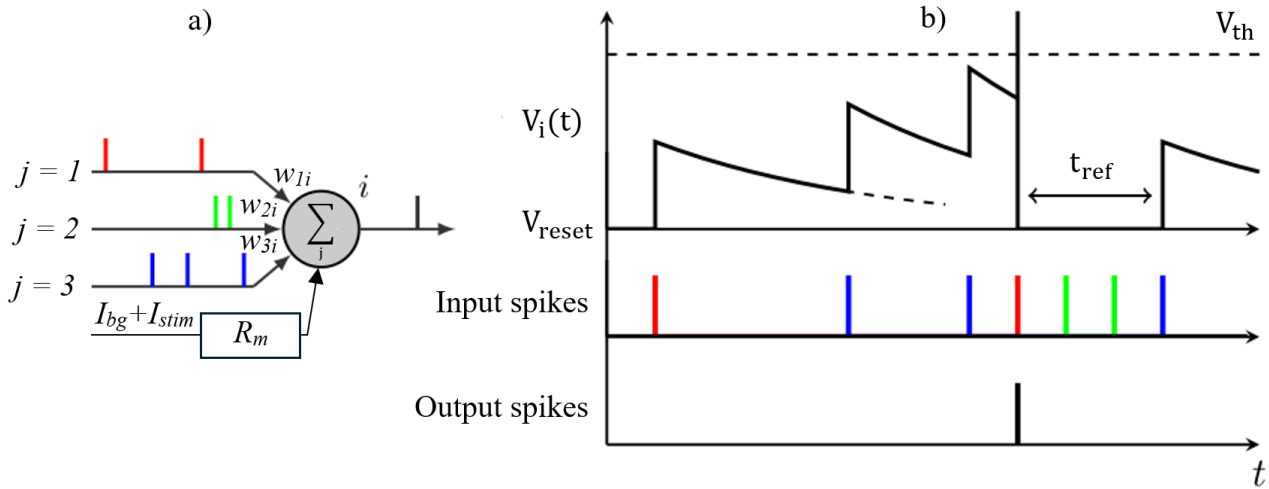


Figure 2: The behaviour of the LIF neuron. (a) A schematic of the LIF neuron model depicting the input spikes arriving to neuron  $i$  from neurons  $j$  via synapses of weight  $w_{ji}$ , and the input stimulation  $I_{stim}$  and background  $I_{bg}$  currents. The sum of these contributions causes neuron  $i$  to spike, represented by the black spike exiting the neuron. (b) The membrane voltage  $V_i(t)$  and the output spikes of neuron  $i$  in response to a set of input spikes from presynaptic neurons  $j$ . In this figure  $V_{rev} = V_{reset}$ . Figure adapted from [20].

## 2.2 Synaptic tagging and capture

The STC hypothesis is a biologically plausible learning rule, providing a possible explanation of the mechanisms underlying memory storage and recall in the mammalian neocortex [11, 21, 22, 23]. The hypothesis describes the mechanisms by which synaptic weights change, altering the strength of connections between the neurons within our brains. Through the continual altering of these synaptic weights, memories are consolidated within neural networks through the formation of Hebbian cell assemblies [11]. These are clusters of neurons displaying strong synaptic connections, linking their activations. Stimulation of a portion of neurons within a Hebbian cell assembly can cause the entire assembly to spike, resulting in memory recall. This behavior can be leveraged to train neural networks to recall specific memories in response to distinct inputs [11, 19].

A critical aspect of the STC hypothesis is its operation on two distinct phases: the early- and the late-phases of long-term synaptic changes (also referred to as long-term synaptic plasticity). The early-phase describes synaptic weight changes that only last a few hours; they decay to their equilibrium values in the absence of further change-inducing inputs [11]. For the influence of the early-phase weight (EPW) changes of a synapse to be maintained, a consolidation process must occur. This consolidation process involves the change of the synapse's late-phase weight (LPW). For the LPW of a synapse to change, the EPW must meet the conditions required for a synaptic tag to be formed at the synapse, allowing it to capture protein. Protein capture at a synapse is necessary for changes in its LPW to take place [11]. The LPW configuration of a synapse is stored indefinitely [21], and is added to the EPW to produce the total synaptic weight [12].

An example of the behaviour of a synapse's weight over time, as determined by STC, is illustrated in Figure 3, which depicts the response of the synaptic weight following a rapid increase in the EPW at  $t = 0$ . The response demonstrates the operation of the two separate phases, with the EPW decaying

to its reference value over a seven hour period, and the LPW consolidating the initial change to the EPW.

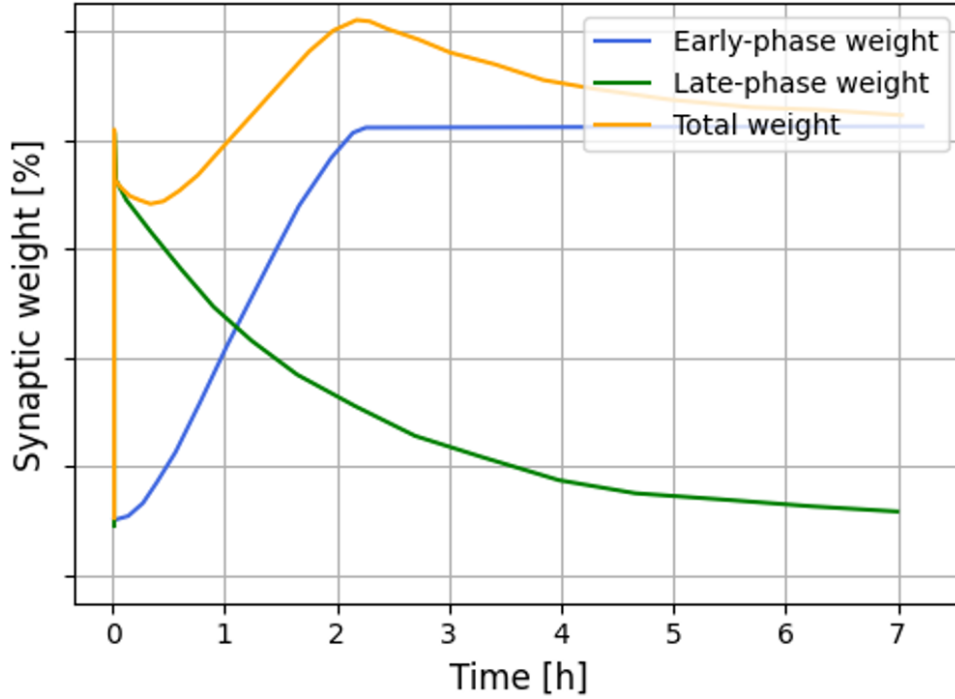


Figure 3: The behaviours of the EPW, LPW and total weight to an intensive period of pre- and postsynaptic spikes from  $t = 0$  s to  $t = 0.2$  s, as determined by STC. The EPW grows during the 0.2 s time interval during which neurons are spiking, and then decays once the spiking stop. During this decay, the LPW grows, consolidating the changes to the EPW. This consolidation only occurs because the change in the EPW met the necessary conditions, which are explained in more detail in Section 2.2.3. Figure adapted from [11].

### 2.2.1 Calcium concentration

The working principles of STC can be split into three subsections. The first is the response of the calcium concentration at the synapse, which ultimately determines the early-phase and thus late-phase responses. The calcium concentration response is driven by pre- and postsynaptic spikes of the neurons at either end of the synapse, as given by [12]:

$$\frac{d}{dt}c_{ji}(t) = -\frac{c_{ji}(t)}{\tau_c} + c_{\text{pre}} \sum_n \delta(t - t_j^n - t_{c,\text{delay}}) + c_{\text{post}} \sum_m \delta(t - t_i^m), \quad (2)$$

with  $c_{ji}(t)$  the calcium concentration at the postsynaptic site;  $\tau_c$  the calcium time constant;  $c_{\text{pre}}$  and  $c_{\text{post}}$  the increase in the calcium concentration due to a pre- and postsynaptic spike, respectively;  $t_j^n$  and  $t_i^m$  the pre- and postsynaptic spike times, respectively; and  $t_{c,\text{delay}}$  the delay in the calcium concentration response after a presynaptic spike.

The first term on the right-hand side of Equation (2) results in the exponential decay of the calcium concentration to zero, whereas the second and third terms give the contributions of pre- and postsynaptic spikes to the calcium concentration, respectively. The behaviour elicited by Equation (2) is depicted in Figure 4.

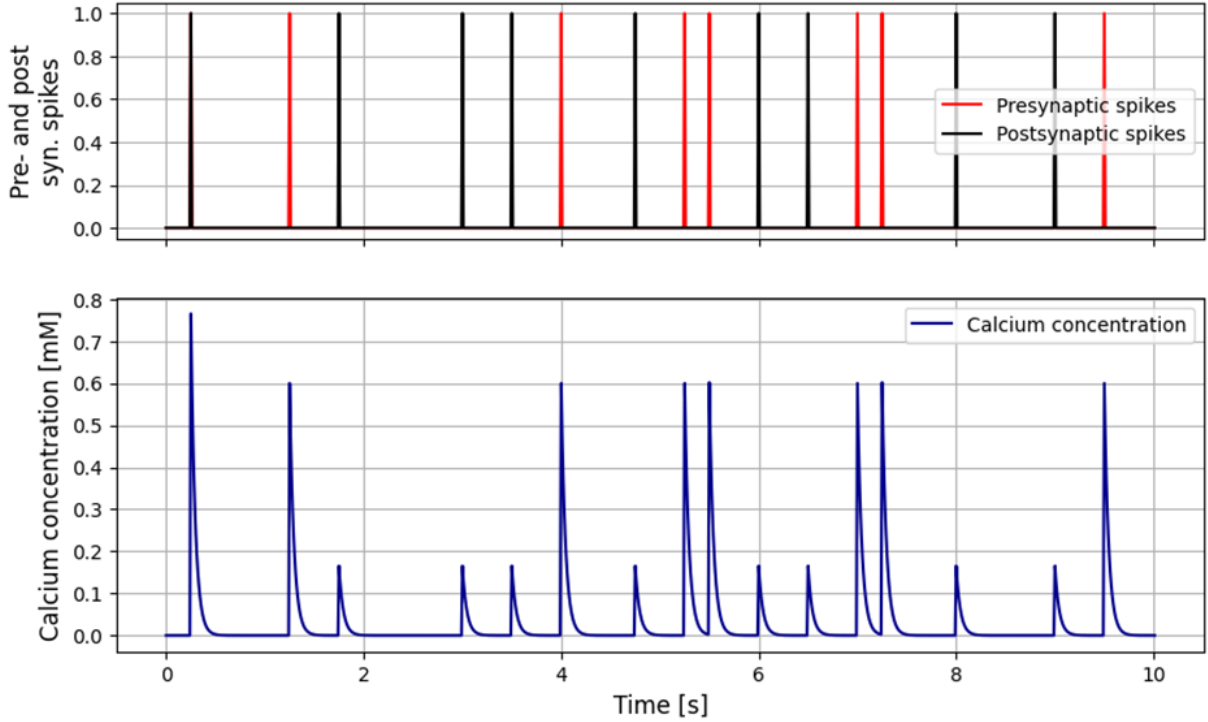


Figure 4: The behaviour of the calcium concentration at the postsynaptic site in response to the presence of pre- and postsynaptic spikes. The behaviour shows a distinct increase in the calcium concentration in response to each type of spike, followed by exponential decay.

### 2.2.2 Early-phase weight

The calcium concentration then determines the behaviour of the EPW of the synapse. The EPW refers to changes in the synaptic weight that last a few hours [11]. The behaviour of the EPW  $h_{ji}(t)$  is described by [12]:

$$\tau_h \frac{dh_{ji}(t)}{dt} = 0.1(h_0 - h_{ji}(t)) + \gamma_p \cdot (h_{max} - h_{ji}(t)) \cdot \Theta(c_{ji}(t) - \theta_p) - \gamma_d \cdot h_{ji}(t) \cdot \Theta(c_{ji}(t) - \theta_d). \quad (3)$$

Here,  $\tau_h$  is the early-phase time constant;  $h_{ji}$  the reference/equilibrium value of the EPW;  $\gamma_p$  and  $\gamma_d$  the potentiation and depression strengths, respectively;  $h_{max}$  the maximum value of the EPW;  $\Theta(\cdot)$  the Heaviside function; and  $\theta_p$  and  $\theta_d$  the potentiation and depression thresholds, respectively.

Equation (3) illustrates the three ways in which the EPW is updated: potentiation, depression and recovery. Potentiation and depression refer to the rapid increase and decrease in the EPW, as a result of the calcium concentration surpassing the potentiation and depression thresholds. The behaviour of these mechanisms is given by the second and third terms on the right-hand side of Equation (3); potentiation and depression respectively. The depression threshold  $\theta_d$  is lower than the potentiation threshold  $\theta_p$ , which means that if potentiation is occurring, so is depression. However,  $\gamma_p$  is roughly five times the magnitude of  $\gamma_d$ , making potentiation the dominant mechanism in this scenario. Finally, the recovery term  $0.1(h_0 - h_{ji}(t))$  describes the exponential return of the EPW to its reference value. Recovery is always active, but is two orders of magnitude weaker than both potentiation and depression [11, 12]. Figure 5 demonstrates the behaviour of the EPW in response to changes in the calcium

concentration.

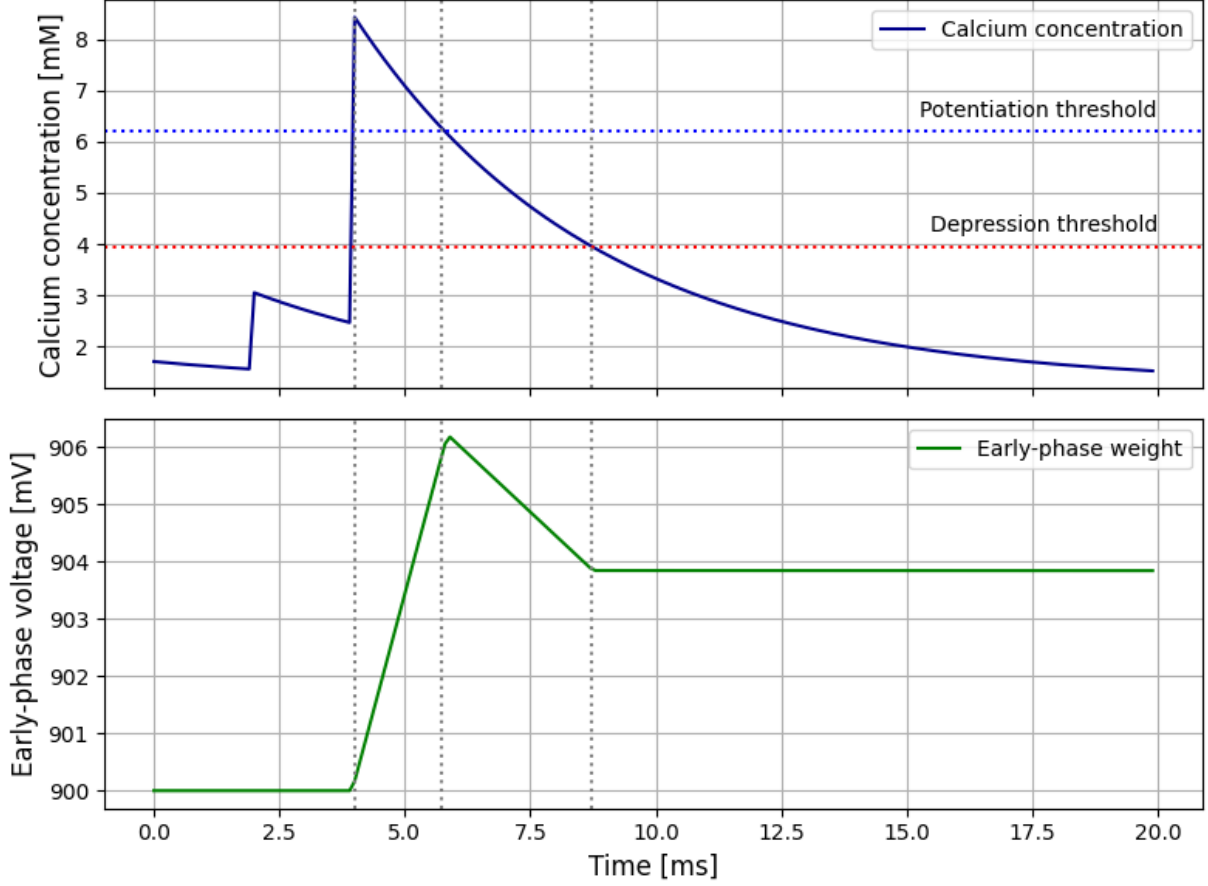


Figure 5: The behaviour of the EPW in responses to changes in the calcium concentration. Potentiation of the EPW is visible during the time interval in which the calcium concentration is above the potentiation threshold (from 4.0 s to 5.9 s), and depression is visible during the time interval the calcium concentration is between the potentiation and depression thresholds (from 5.9 s to 8.4 s). Although always active, recovery is not visible in this figure. This is due to the magnitude of the early-phase time constant (688.4 s), which makes recovery a slow process that cannot be observed on the millisecond timescale.

### 2.2.3 Late-phase weight

The behaviour of the EPW dictates the response of the synapse's LPW. A sufficient deviation of the EPW from its reference value triggers the formation of a synapse-specific tag, leading to the capture of proteins in the synapse (hence the name synaptic tagging and capture [11]). The concurrence of a synaptic tag and sufficient protein availability results in changes to the LPW. This process is described by [11]:

$$\tau_z \frac{dz_{ji}(t)}{dt} = p_i(t) \cdot (1 - z_{ji}(t)) \cdot \Theta((h_{ji}(t) - h_0) - \theta_{\text{tag}}) - p_i(t) \cdot (z_{ji}(t) + 0.5) \cdot \Theta((h_0 - h_{ji}(t)) - \theta_{\text{tag}}). \quad (4)$$

Here,  $z_{ji}$  is the LPW variable;  $\tau_z$  is the late-phase time constant; and  $\theta_{tag}$  the tagging threshold that must be surpassed for the formation of a synaptic tag. The first term on the right-hand side of the equation describes late-phase potentiation, and the second term describes late-phase depression. The protein availability  $p_i(t)$  at the postsynaptic site is determined based on the sum of the EPW change across all the synapses  $j$  connected to this site, as given by [12]:

$$p_i(t) = \begin{cases} \alpha & \text{if } \sum_j |h_{ji}(t^*) - h_0| > \theta_{pro} \text{ at any } t^* \leq t, \\ 0 & \text{else.} \end{cases} \quad (5)$$

For late-phase potentiation or depression to occur at synapse  $i$ , the sum of the absolute value of the change in the EPW of all the synapses  $j$  connected to the post-synaptic site of synapse  $i$  must be larger than the protein capture threshold  $\theta_{pro}$ ; i.e.,  $|\sum_j h_{ji}(t^*) - h_0| > \theta_{pro}$ . Once this condition is met, the protein availability becomes  $\alpha$  and stays this way indefinitely. This influence this has on the LPW behaviour is illustrated in Figure 6.

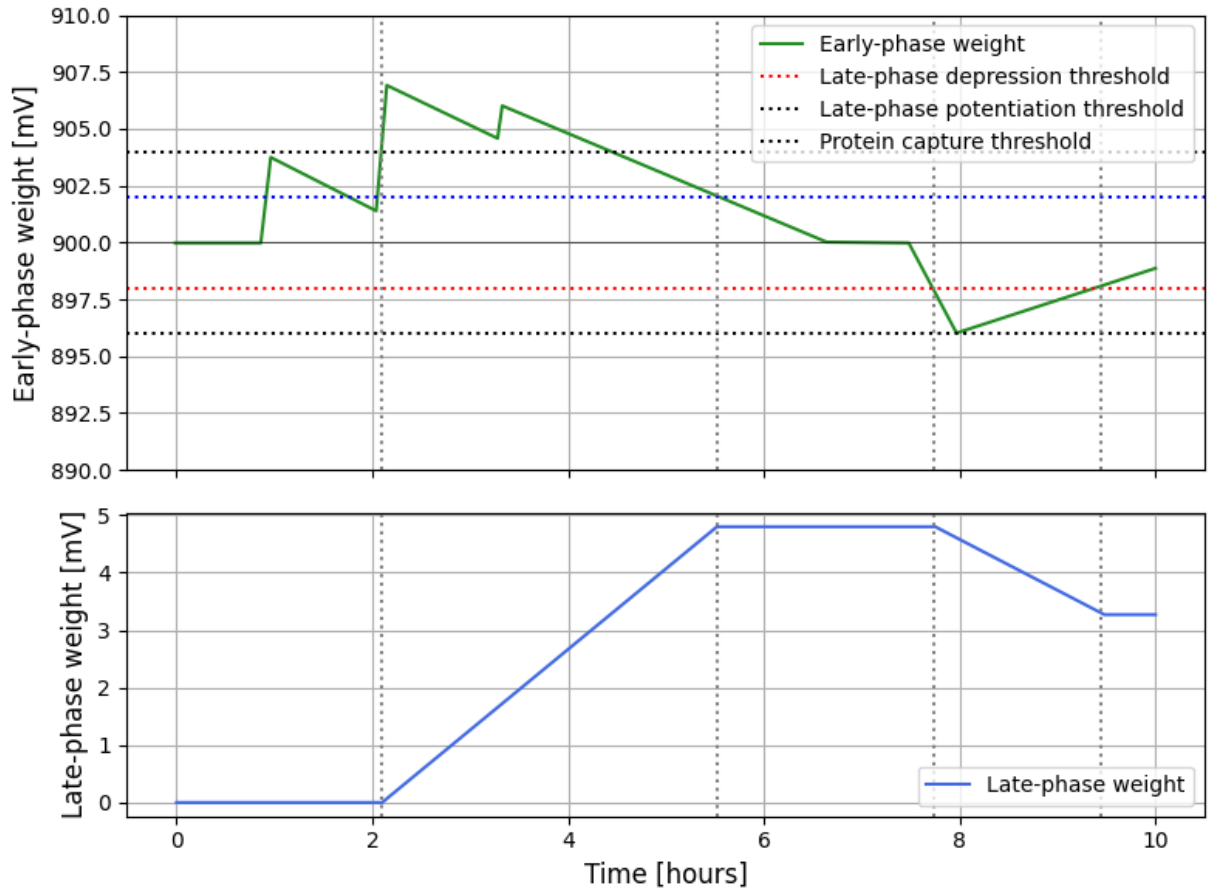


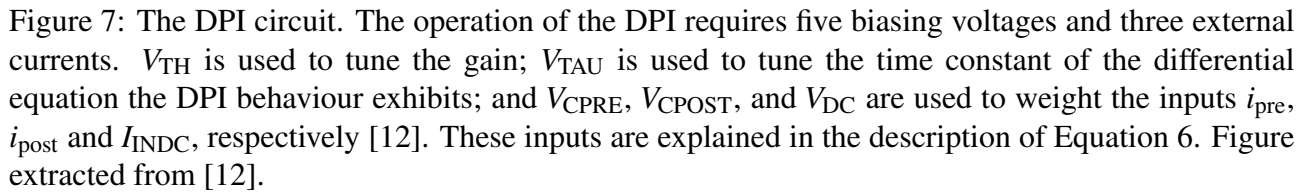
Figure 6: Changes in the LPW in response to changes in the EPW. Before the EPW crosses the protein capture threshold the LPW stays constant, since  $p_i(t) = 0$  (from 0.0 s to 2.1 s). Once this threshold is passed (at 2.1 s), a synaptic tag forms and  $p_i(t)$  is set to  $\alpha$ . The LPW then potentiates when the EPW is above the potentiation threshold (from 2.1 s to 5.5 s), and depresses when the EPW is below the depression threshold (from 7.7 s to 9.4 s). Unlike the EPW, the LPW does not recover.

## 2.3 Implementation of STC in the CMOS circuits

This work evaluates the implementation of STC in the CMOS circuits proposed in [12] through emulating the behaviour of the circuits in a Python environment. This work then uses the Python code to simulate the behaviour of the circuitry on a network level. This subsection provides an overview of how the circuitry executes the differential equations governing STC presented in the previous subsection, focusing only on the calcium and early-phase portions of the circuits. The explanation of the implementation of the late-phase calculation is excluded, as the code produced in this work uses Equation (4), rather than mimicking the late-phase circuitry. The reasons for this stem from the fact that this portion of the circuit is likely to be evaluated with emerging devices in future iterations of the CMOS circuits, alongside the relative complexity of the late-phase circuitry. This is described in more detail in the *Discussion*.

### 2.3.1 Calculation of the calcium concentration in the CMOS circuits

A differential pair integrator (DPI) [24] is used to perform the calcium concentration calculations described in Equation (2). The DPI is a current-mode circuit [25], that receives voltage pulses as inputs and outputs a current. The voltage pulses are used to communicate input spikes to the CMOS synapse, and the output current is used as an indicator of the calcium concentration in the synapse [12]. A schematic of the DPI is provided in Figure 7.


$$\frac{d}{dt}i_{ca} = \frac{1}{\tau_{DPI}}(-i_{ca} + \frac{I_{TH}}{I_{TAU}}(i_{pre} + i_{post} + I_{INDC})). \quad (6)$$

### 2.3.2 Calculation of the early-phase weight in the CMOS circuits

The output current  $i_{ca}$  of the DPI is fed into the early-phase portion of the CMOS circuits, consisting of a control block [12], two winner-take-all circuits [26, 27], three ultra low leakage blocks [12] and a capacitor. The early-phase circuit takes  $i_{ca}$  as an input and calculates the EPW based on Equation (3),



outputting the EPW as the voltage  $v_h$ . The voltage  $v_h$  is then fed back into the input of the early-phase circuit, allowing the circuit to perform the recovery term of Equation (3). The logic extracted from the early-phase circuit is presented by the block diagram in Figure 8.

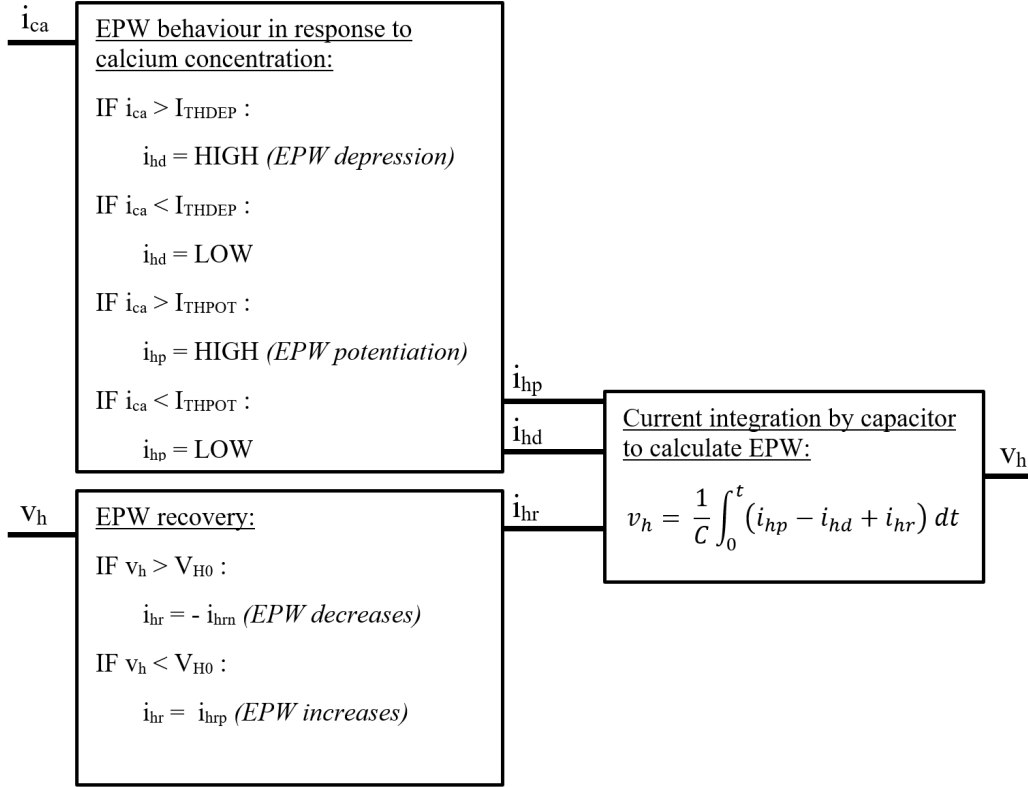


Figure 8: A block diagram illustrating the logic extracted from the early-phase portion of the synapse circuits.  $i_{ca}$  is the current indicating the calcium concentration;  $I_{THPOT}$  and  $I_{THDEP}$  are the potentiation and depression thresholds, respectively;  $i_{hp}$  and  $i_{hd}$  are the potentiation and depression currents, respectively;  $i_{hr}$  is the recovery current;  $i_{hrm}$  is the magnitude of the recovery current when the EPW is above its reference value  $V_{H0}$ ;  $i_{hrp}$  is the magnitude of the recovery current when the EPW is below its reference value  $V_{H0}$ ; and  $C$  is the capacitance of the capacitor used to perform the integral of the potentiation, depression and recovery currents.

The block diagram in Figure 8 consists of three blocks. The first (top left) compares the calcium concentration to the early-phase potentiation and depression thresholds, and depending on this comparison, sets the potentiation and depression currents to either high or low. When the current is set to high, it means the corresponding mechanism is active. The second block (bottom left) sets the recovery current  $i_{hr}$  to either a positive value  $i_{hrp}$  or negative value  $-i_{hrm}$  depending on whether the EPW voltage  $v_h$  currently lies above or below the reference value  $V_{H0}$ , determining the direction and magnitude of EPW recovery. Finally, the integral of the potentiation  $i_{hp}$ , depression  $i_{hd}$  and recovery currents  $i_{hr}$  is performed using a capacitor, accounting for the negative contribution to the EPW that depression should cause. The result of this integral produces  $v_h$ .

## 3 Results

### 3.1 Summary of methods

This work reproduces the behaviour of a CMOS implementation of a synaptic model, performing the biologically inspired multi-timescale learning rule STC, in a Python environment. To validate the accuracy of this replication, an additional Python script was produced, based on the differential equations governing STC. A comparison of the two scripts was performed, verifying that the circuit-based script performs STC.

The output of the circuit-based script was also compared to simulations of the circuitry itself, performed in Cadence Virtuoso, testing whether the similarity was sufficient to use the Python code to analyse the performance of the CMOS circuits at a network level. As these comparisons both yielded satisfactory results, the Python code was then incorporated into a two-layer feedforward SNN, which was trained and tested using the MNIST dataset.

The following subsections present the results of the aforementioned comparisons, displaying the similarity of the code output with regard to the CMOS circuits, which is in supporting the claim that the synapse circuitry functions on a network level.

### 3.2 Reproduction of the synapse circuits in Python

The code reproducing the CMOS implementation of the synapse was written based on the logic extracted from the circuits, as presented in the *State of the Art*. The calcium concentration updates, in response to pre- and postsynaptic spikes, were calculated using Equation (6), and the early-phase weight calculation was executed using the logic displayed in the block diagram in Figure 8. However, as mentioned in Section 2.3, the late-phase portion of the code deviates from the circuitry, solving Equation (4), rather than performing a direct implementation of the circuit logic. More detail on this can be found in the *Discussion*.

The code was written in Python 3.10, using the Google JAX framework and the Equinox library. The complete code is displayed in Appendix A.

#### 3.2.1 Testing of the synapse circuit-based script

To test the code reproducing the synapse circuits, another script was written based purely on the differential equations governing STC (Equations 2, 3 and 4), solving them using the forward Euler method. This script served as a control: it exhibits the behaviour of the differential equations that the circuitry is based on. Comparisons between the two Python scripts were then performed to verify that the circuit reproduction does perform STC as intended. One such comparison is depicted in Figure 9, illustrating the response of the two scripts to a random array of pre- and postsynaptic spikes. The difference in the time scale is a result of the acceleration factor of ten implemented in the CMOS model, which was applied to relax circuit design constraints [12].

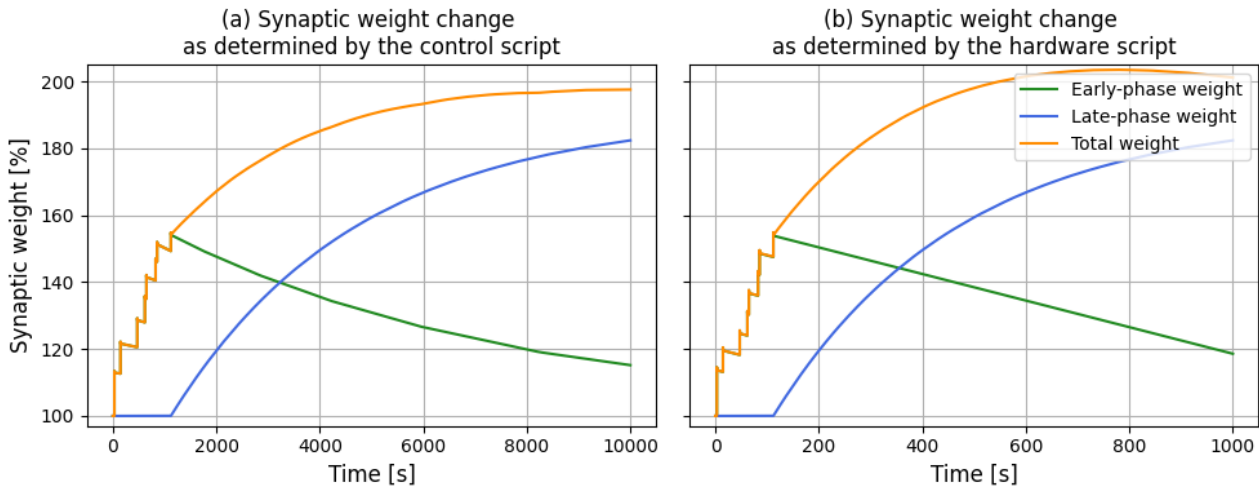


Figure 9: The output of the control script (a) and the circuit-based script (b) in response to an identical test input consisting of randomly distributed pre- and postsynaptic spikes in the first tenth of the time interval (from 0 to 1000 s in (a), and from 0 to 100 s in (b)), followed by an absence of spikes. The circuit-based code can be found in Appendix A, the differential equation-based code in Appendix B and the constants used to produce these figures can be found in Appendix C. The code used to produce this figure, alongside all other relevant figures can be accessed via the link provided in Appendix E.

The comparison of the two scripts illustrated in Figure 9 was used to substantiate the correct functionality of the circuit replication, as both codes exhibit the defining characteristics of STC at the appropriate times. Potentiation - the steep increase in the EPW - is observed during the interval in which pre- and postsynaptic spikes are present, as these spikes cause the calcium concentration to surpass the potentiation threshold. The drop following each of the potentiations is due to both depression and EPW decay. The two mechanisms are distinguishable by the rate of the decrease they elicit. Figure 10 presents an enlarged depiction of one of the potentiation spikes in Figure 9, clearly illustrating the two different gradients in the decline of the EPW. The steeper of the two is depression, caused by the brief period during which the tail of the calcium concentration has decayed to below the potentiation threshold, but is still above the depression threshold. The sudden leveling out of the gradient occurs once the calcium concentration decays beyond the depression threshold, and the only contribution to the EPW is its recovery towards its steady state.

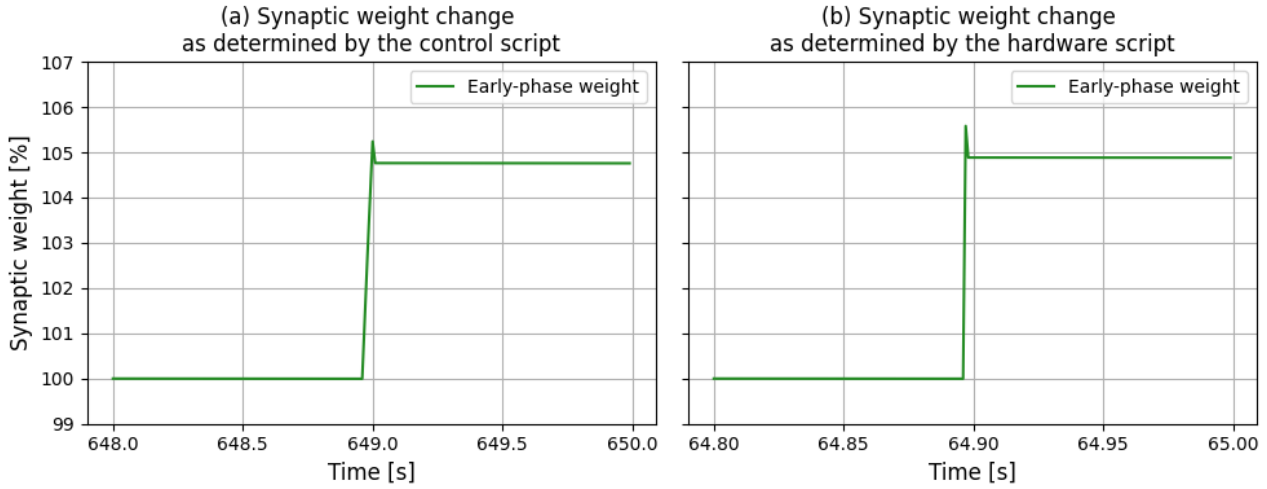


Figure 10: An enlarged version of the EPW, focusing on its behaviour directly after potentiation occurs. Although the effects of depression are clearly visible in this figure (the steep drop in the EPW), the effects of EPW decay/recovery are not. This is merely due to the narrow time window used, relative to the time constant determining this decay (688.4 s for (a) and 68.84 s for (b)).

Aside from the timescale, the only major difference in the behaviours of the two codes is that in the script based on the circuits, recovery is linear, whereas in the script based on the equations it is exponential. This difference arises from the circuitry itself, rather than from an oversight in one of the two codes. The circuits calculate the rate of recovery by integrating the recovery current over time. This current is either one of two values: a fixed negative value or a fixed positive value, depending on whether the EPW is above or below the EPW reference value. Hence, the integration of the recovery current over time produces a linear response, rather than the exponential decay observed in the behaviour of the differential equation the CMOS circuits are based on. The justification for this approximation is the magnitude of the early-phase time constant: it is large enough that a linear EPW recovery is not a problematic difference.

In addition to potentiation, depression and recovery, consolidation is also observed in Figure 9, with the initiation of changes to the LPW demonstrating the presence of a synaptic tag. This means the EPW change has exceeded the tagging threshold. In the example presented in Figure 9, this threshold is reached just as the synaptic spikes stop. Hence, as the EPW decays, it is consolidated by means of long-term potentiation of the LPW. It is worth noting that if the test input had resulted in the EPW being depressed beyond the tagging threshold, this would be consolidated by long-term depression of the LPW.

### 3.2.2 Comparison of the circuit-based script to literature

To further investigate the accuracy of the circuit-based script in simulating the CMOS implementation of the STC-based synapse, the code was compared to both previously conducted simulations of the CMOS circuits and the results of the STC simulations published in [11]. Previous simulations of the circuits were performed Cadence Virtuoso [12], whereas the results in [11] were determined using a C++ script written to solve the differential equations governing STC.

Figure 11 depicts the response of an STC-based synapse to a short period of intense potentiation. Figures 11 (a) and 11 (c) are the outputs of the circuit-based script produced in this work, with the

EPW recovery accelerated by a factor of 32 and 7.2, respectively. The acceleration factor of 32 was chosen to match the Cadence simulation, presented in Figure 11 (b). Figure 11 (c) was included to demonstrate that reducing the acceleration factor used in the circuit-based script exaggerates the curve in the total synaptic weight, which is observed in both Figures 11 (b) and 11 (d), with 11 (d) presenting the results of the simulations performed in [11].

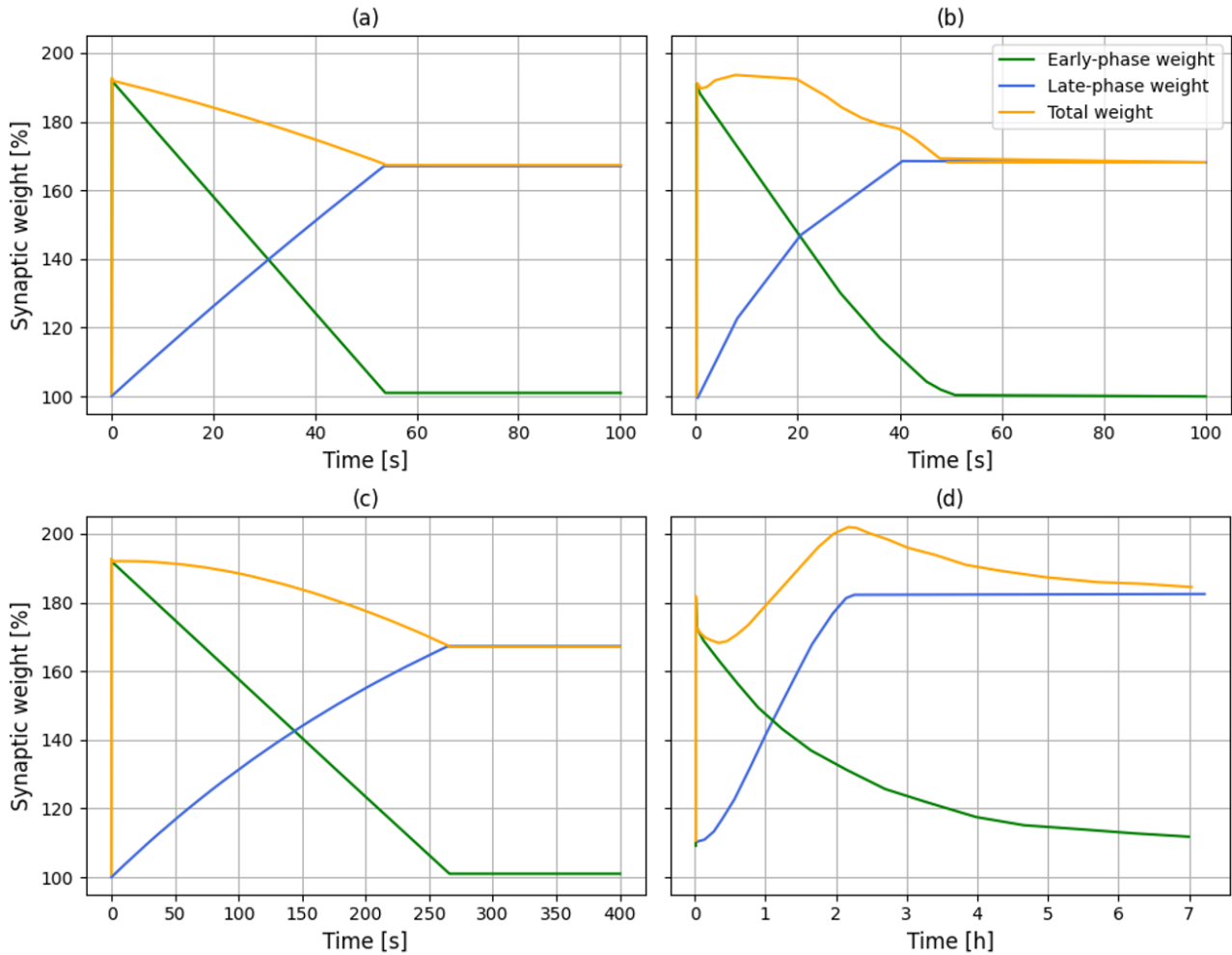


Figure 11: Four simulations of the response of the synaptic weight to a strong potentiation 0.2 s-long at  $t = 0$ . (a) The output of the circuit-based script produced in this work, using an acceleration factor of 32 for the EPW decay. (b) The results produced by a simulation of the synapse circuits in Cadence Virtuoso, using an acceleration factor of 32 for the EPW decay. The data presented is extracted from [12]. (c) The output of the circuit-based script produced in this work, using an acceleration factor of 7.2 for the EPW decay. (d) An adaptation of the figure presenting the output of the simulation performed in [11].

Although there are observable differences in the behaviours illustrated in the four sub-figures, they are comparable. If the acceleration factor used in (c) is accounted for, then the responses in (a), (b) and (c) all exhibit activation of the same STC mechanisms at the appropriate times: potentiation during the 0.2 s-long spiking interval at the start of the simulation; recovery of the EPW once the spiking input ends; and consolidation of the EPW by means of potentiation of the LPW, which indicates the development of a synaptic tag during the EPW potentiation, leading to protein capture at the synapse.

Sub-figure (d) is somewhat of an outlier, but this is logical, as this work aims to replicate the CMOS circuits exhibiting the behaviour in Figure 11 (b), not the exact behaviour illustrated in 11 (d). The simulations performed to obtain the results in (d) used slightly different differential equations to the ones implemented in the circuitry, with the latter omitting two terms in the equation determining the EPW, specifically a term dictating calcium-dependent fluctuations and a term enforcing two 'special plasticity conditions' [12, 11]. The simulations performed in [11] have only been included to serve as a reference point for the expected circuit behaviour, as they exhibit the 'targeted behaviour' [12] of the CMOS circuits replicated in Python by this work.

The comparability of the behaviours depicted in Figures 11 (a), (b) and (c) indicates that the extent to which the circuit-based Python script accurately replicates the behaviour of the CMOS circuits is sufficient. It meets the requirements to which this work will be subjected, as this work serves as a proof-of-concept, rather than an exact simulation of the circuits. The justification for not needing an exact simulation as of yet is detailed in the *Discussion*.

### 3.3 Creation of an SNN to investigate the behaviour of the synapse circuitry at a network level

Once it had been verified that the circuit-based Python script was a sufficiently accurate replica of the CMOS circuits, the code was used to simulate the circuitry on a network level. This was achieved by creating an SNN using the circuit-based Python script and then training and testing the network using the MNIST dataset. The MNIST dataset is a database of handwritten digits, rasterised onto a  $28 \times 28$  pixel grid, with each pixel being assigned an intensity value, ranging from values of 0 to 255 [28]. A visual explanation of this encoding process is depicted in Figure 12.

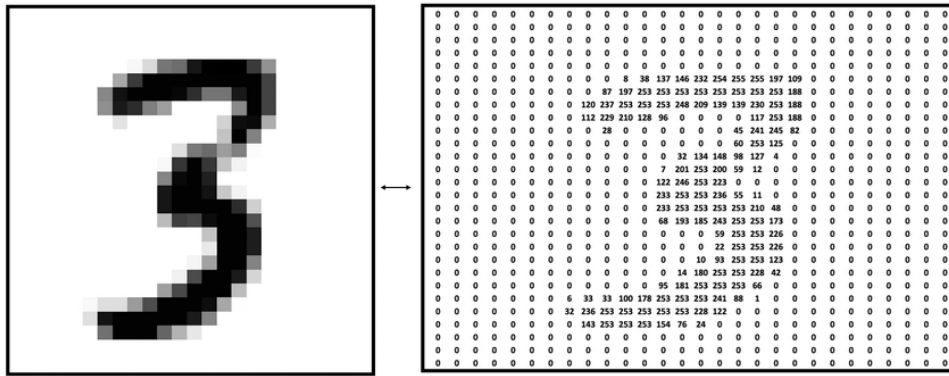


Figure 12: The encoding of a handwritten '3' as an MNIST sample. Figure extracted from [29].

#### 3.3.1 Network architecture

The SNN created comprises a two-layer, feedforward structure, as depicted in Figure 13. The input layer contains 784 neurons, one for each pixel of the  $28 \times 28$  grid. Each neuron in the first layer is connected by an STC synapse to each output neuron in the second layer. The number of output neurons varied, matching the number of digits the network was being trained to identify (e.g. if the network was only being trained to identify ones and zeros, there were only two output neurons). Each output neuron has two sources of input: the input spikes delivered via the synapses from the first

layer neurons and secondly, a stimulus input in the form of a stimulation current, active only during the training of the network. The network uses LIF neurons, which were implemented in the code by solving Equation 1 in discrete time using the forward Euler method.

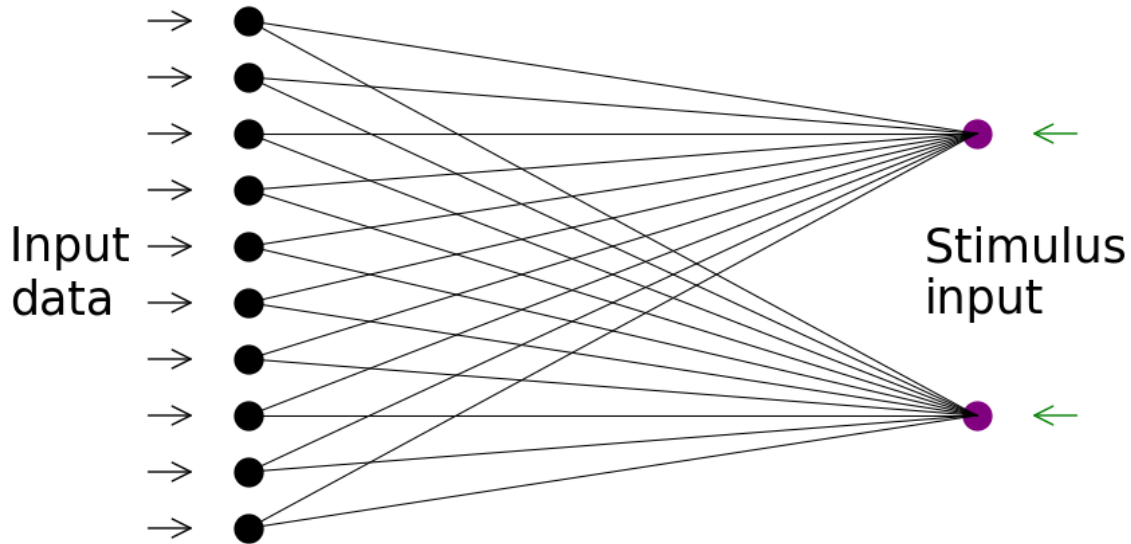


Figure 13: A two-layer, feedforward neural network with input neurons on the left and output neurons on the right. This figure only illustrates ten of the 784 neurons in the first layer for improved clarity. Arrows on the left represent the MNIST input data, whereas arrows on the right represent the stimulus input.

### 3.3.2 Training and testing

To train the network, the input data was first rate-encoded, meaning information was communicated by neurons through making use of different spiking frequencies. A linear translation was used, projecting the pixel intensities onto a range of firing rates starting at 0 Hz (corresponding to a pixel intensity of zero) and ending at 40 Hz (for the maximum pixel intensity value of 255). The 40 Hz limit was chosen to keep firing rates within a biologically plausible range [30].

During training, each sample was presented to the network for 150 ms, followed by a 200 ms phase absent of any spikes, allowing all neuron membranes to decay to their resting values. Each 150 ms phase was accompanied by a 1 nA stimulation current pulse sent to the second layer neuron matching the label of the sample being presented, and a -1 nA inhibition current sent to all other second layer neurons. The purpose of the stimulatory/inhibitory current pulses is to ensure only the correct second layer neuron fires for each sample presented, i.e., the second layer neuron matching the label of the sample being presented. This winner-take-all mechanism is a computationally efficient way to implement the behaviour of inhibitory neurons. It ensures that for each sample labelled 'X' presented to the network, only the synapses connecting the firing input neurons and the output neuron labelled 'X' experience both pre- and postsynaptic spikes. All other synapses experience either no spiking, or *only* either pre- or postsynaptic spikes.

Minor adjustments were made to the currents and thresholds defining the behaviour of the synapse (the updated variables can be found in Appendix D), such that the presence of both a pre- and postsynaptic spike at a synapse would result in potentiation, and the presence of only one of the two would result in depression. As a result, the synapses connecting the neurons in the first layer (that tend to spike for input 'X') and neuron 'X' in the second layer strengthen, whereas all other connections weaken. Hence, the second layer neuron 'X' becomes far more likely to spike when a sample 'X' is presented to the network in future, allowing the network to distinguish between different inputs. This process is visualised in Figure 14.



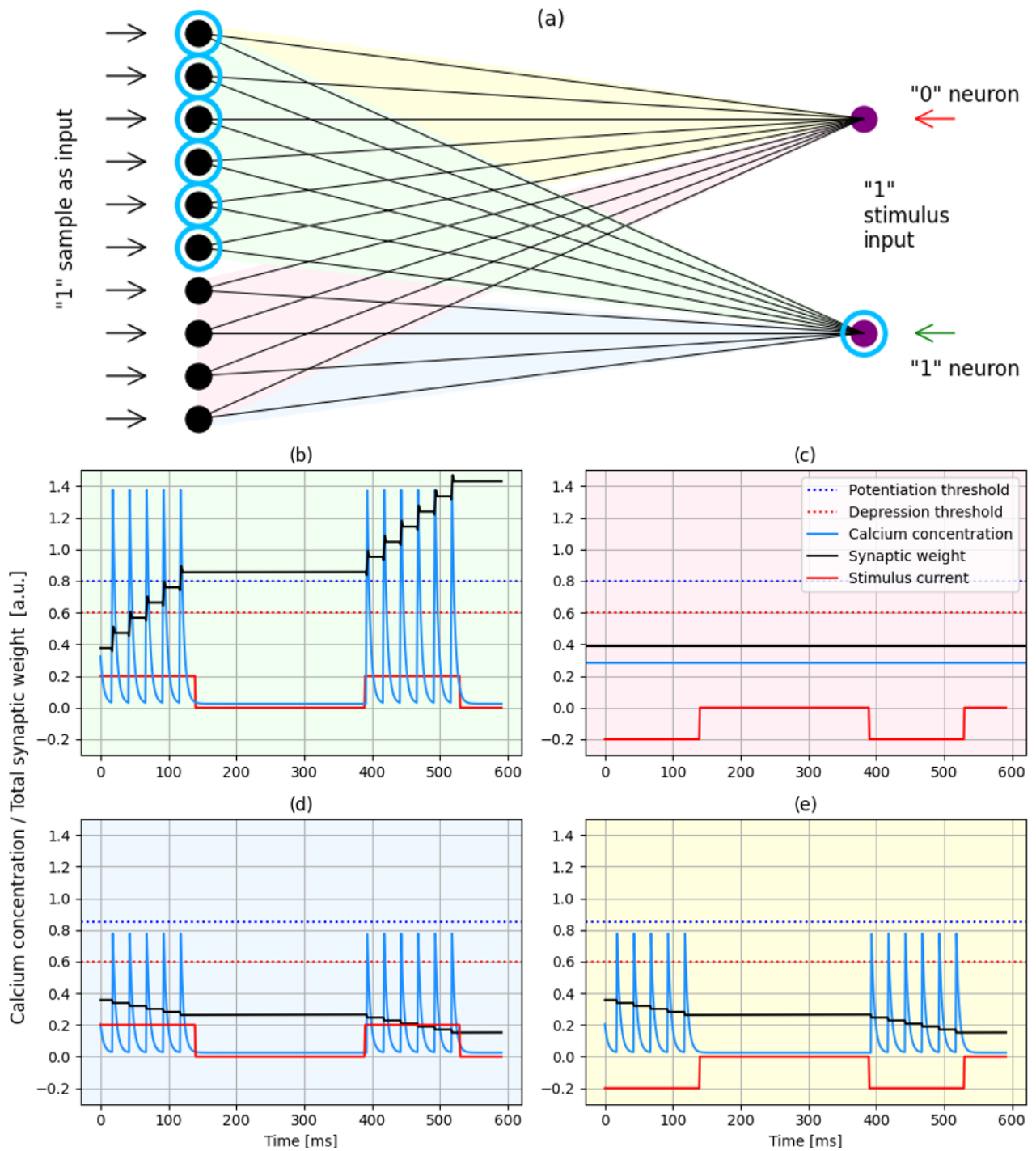


Figure 14: (a) The network architecture, highlighting the four possible groups of synapses. The network is being presented with an example input sample labelled '1'. Blue rings indicate firing neurons, the green arrow indicates a stimulatory current and the red arrow an inhibitory current. (b) The presence of both pre- and postsynaptic spikes at a synapse causes the calcium concentration to surpass the potentiation threshold, leading to an increase in synaptic weight. The solid red line indicates the stimulus input, which can be either positive (stimulatory) or negative (inhibitory). (c) There is no change in synaptic weight if neither pre- nor postsynaptic neurons fire. (d) The presence of *only* postsynaptic spikes causes the calcium threshold to surpass the depression threshold, but not the potentiation threshold, leading to a decrease in synaptic weight. (e) The presence of *only* presynaptic spikes causes the calcium threshold to surpass the depression threshold, but not the potentiation threshold, leading to a decrease in synaptic weight.

To test the performance of the neural network, it was trained on a subset of the MNIST dataset containing 170 samples of zeroes and ones and then tested on a separate subset of 100 samples. During testing, synaptic plasticity was disabled, meaning that the synaptic weights could not change. Testing was performed 200 ms after the last training sample was presented. The accuracy of the network was tested in two scenarios: using the standard early- and late-phase time constants (68.84 s and 360.0 s, respectively); and then using an acceleration factor of 32 for both constants. An accuracy of 96% was achieved in the former case, in which the network was not given time for consolidation: i.e. the EPW and LPW were not given sufficient time to undergo any major weight changes between the end of training and testing. In the latter case, the accelerated time constants allowed the network to consolidate the synaptic weight changes that occurred during training by accelerating the decay of the EPW and the potentiation/depression of the LPW. This produced an accuracy of 93%. The differing levels of accuracy demonstrate the multi-timescale nature of STC, illustrating the behaviour of the network on both the short (standard time constants) and long time-scales (accelerated time constants). Heat maps of the synaptic weights for the standard scenario are plotted in Figure 15.

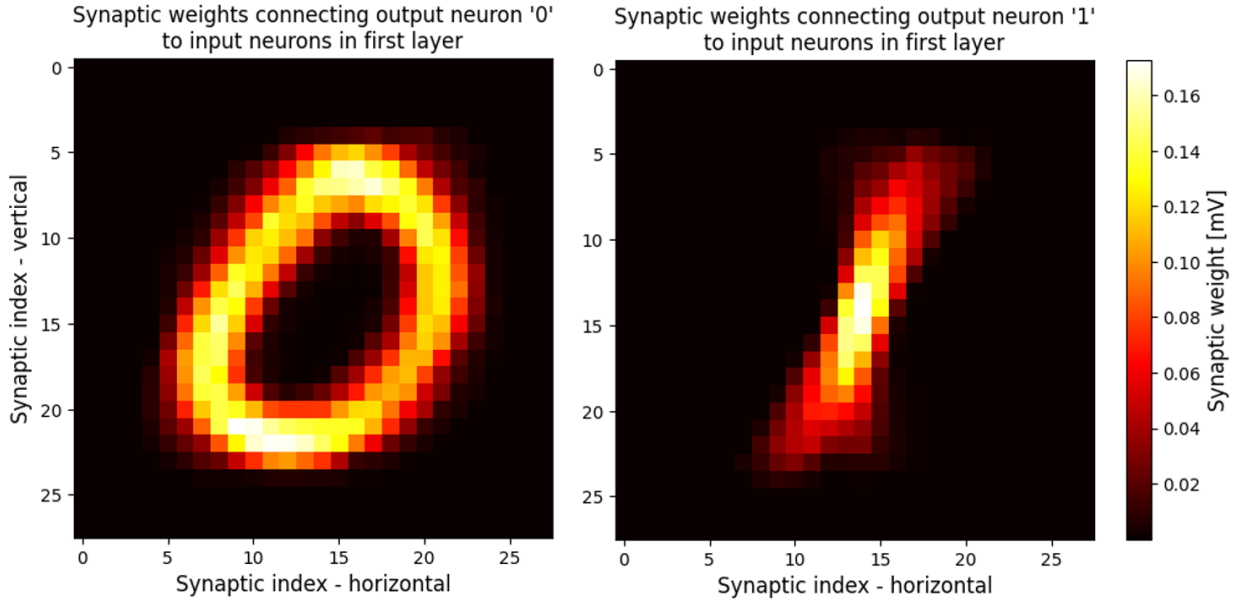


Figure 15: Plot depicting the synaptic weights connecting pre- and postsynaptic neurons after training, but before memory consolidation.

The lowered accuracy for the accelerated time constants can be explained by the drop in total synaptic weight during consolidation, as displayed in Figure 11. Owing to this weight drop, non-zero synaptic weights were on average 9.4% higher in the non-accelerated case. This increased disparity in the weights of connections between a second layer neuron and the first layer neurons helps the network distinguish between the two types of input. Thus, the drop in the total synaptic weight as the network consolidates the changes that occurred during training reduces accuracy, explaining the drop from 96% to 93%.

It is interesting to note that this is the opposite to the behaviour observed in [23], where accuracy improved after consolidation. The explanation for this difference is that synaptic plasticity was disabled during testing in this work, whereas in [23] it was not. When synaptic plasticity is left on, the testing/recall input causes an increase in the EPW. The relative increase in the EPW due to this recall

is much larger once consolidation has taken place, as the EPW has decayed to a much lower level than in the case when the recall stimulus is sent directly after training. If recall is performed directly after training, the EPW has not had a chance to decay, and hence, the total synaptic weight increases by a lower percentage than when testing is done after consolidation. This larger increase in total synaptic weight during recall leads to improved accuracy, explaining why the network becomes more accurate after consolidation. Again, it ought to be emphasized that this only happens when synaptic plasticity is left turned on during testing, which in this work it was not, as the evaluation of the influence of synaptic plasticity during testing is beyond the scope of this paper.

## 4 Discussion

This study demonstrates the compatibility of the CMOS implementation of a synapse, performing the STC learning rule, on a network level. It does this by producing a Python script mimicking the CMOS circuit implementation, and testing the script in a neural network. The validity of the Python script produced was corroborated through comparison of the script to both previous simulations of the synapse circuitry and the differential equations governing STC. The two-layer, feedforward SNN the code was used in achieved an accuracy of 96%, proving the functionality of the synapse circuits on a network level.

It should be noted, however, that the Python script used is not an exact simulation of the CMOS circuits. While the portions of the code responsible for the updates to the calcium concentration and the EPW are derived entirely from the synapse circuitry, the late-phase portion of the code is not. Rather than simulating the circuits, the late-phase portion of the code merely uses the forward Euler method to solve Equation (4), which the late-phase portion of the circuitry is based on. This choice arose from the relative complexity of the late-phase circuitry, which implements late-phase plasticity using a mixed signal approach (both analog and digital), comprising a bump-anti bump circuit [31], two winner-take-all circuits [26, 27], and a control block with a digital counter-oscillator integrator system [12].

To avoid the increase in computational cost the simulation of these components would incur, the code was first written using only Equation (4). The output of the code was then compared to simulations of the CMOS circuits performed in Cadence Virtuoso (Figure 11). Based on these comparisons, it was decided that the behaviour of the code and the circuit simulation matched closely enough, omitting the need to properly replicate the late-phase circuitry in the code. This can be justified further through closer examination of the Cadence Virtuoso simulation producing Figure 11 (b). To reduce simulation times, an 8-bit counter was used in place of the 16-bit counter proposed in the CMOS model, resulting in distinct notches in the slope of the LPW. Had a 16-bit counter been used, the curve would have been smoother, leading to less overestimation of the LPW. This would diminish the prominence of the initial upward slope in the LPW, increasing the similarity of Figure 11 (b) to Figures 11 (a) and (c). Overestimation of the LPW also helps explain why the EPW reaches its maximum value earlier in the Cadence simulation than the Python output, as illustrated in Figure 16.

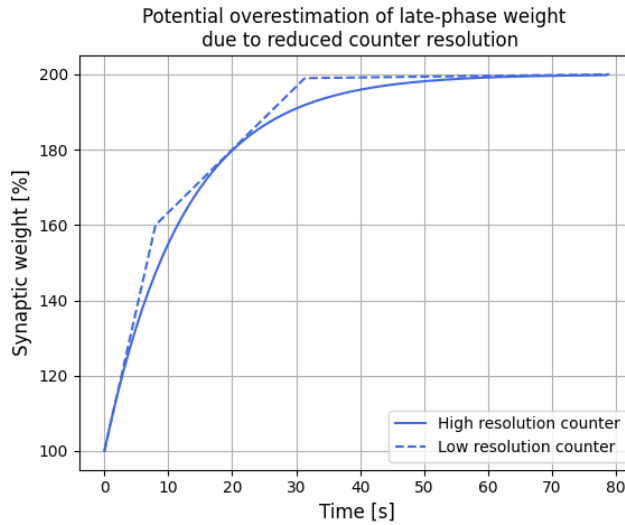


Figure 16: An exaggerated illustration of the potential cause for the larger late-phase contribution in the 8-bit Cadence Virtuoso simulation results in Figure 11(b) relative to the results obtained using the Python script, depicted in Figures 11(a) and (c).

The approach to the late-phase updates is not the only dissimilarity between the circuitry and the Python script aiming to replicate it. Although both the calcium and early-phase portions of the script are based on the CMOS implementation of the synapse, the circuit-based Python code does not simulate the components within the circuits. Instead, the calcium portion of the script implements Equation (6), the differential equation defining the behaviour of the DPI the CMOS synapse uses to calculate the calcium concentration; the code does not replicate each individual transistor and wire the DPI contains, but merely uses the extracted logic to replicate the collective behaviour of all of these components. Likewise, the early-phase portion of the script implements the behaviour of the early-phase circuit, rather than a direct simulation of the components that make up the circuit. Thus, the Python script omits the influence of parasitics owing to the physical characteristics of the circuit layout, such as parasitic capacitances in the various transistors of the circuit [32]. An example of the resulting difference in the Python script and circuit behaviour is illustrated in Figure 17, which depicts the calcium concentration and early-phase response to a post-synaptic spike at 2 ms and a presynaptic spike at 4 ms.

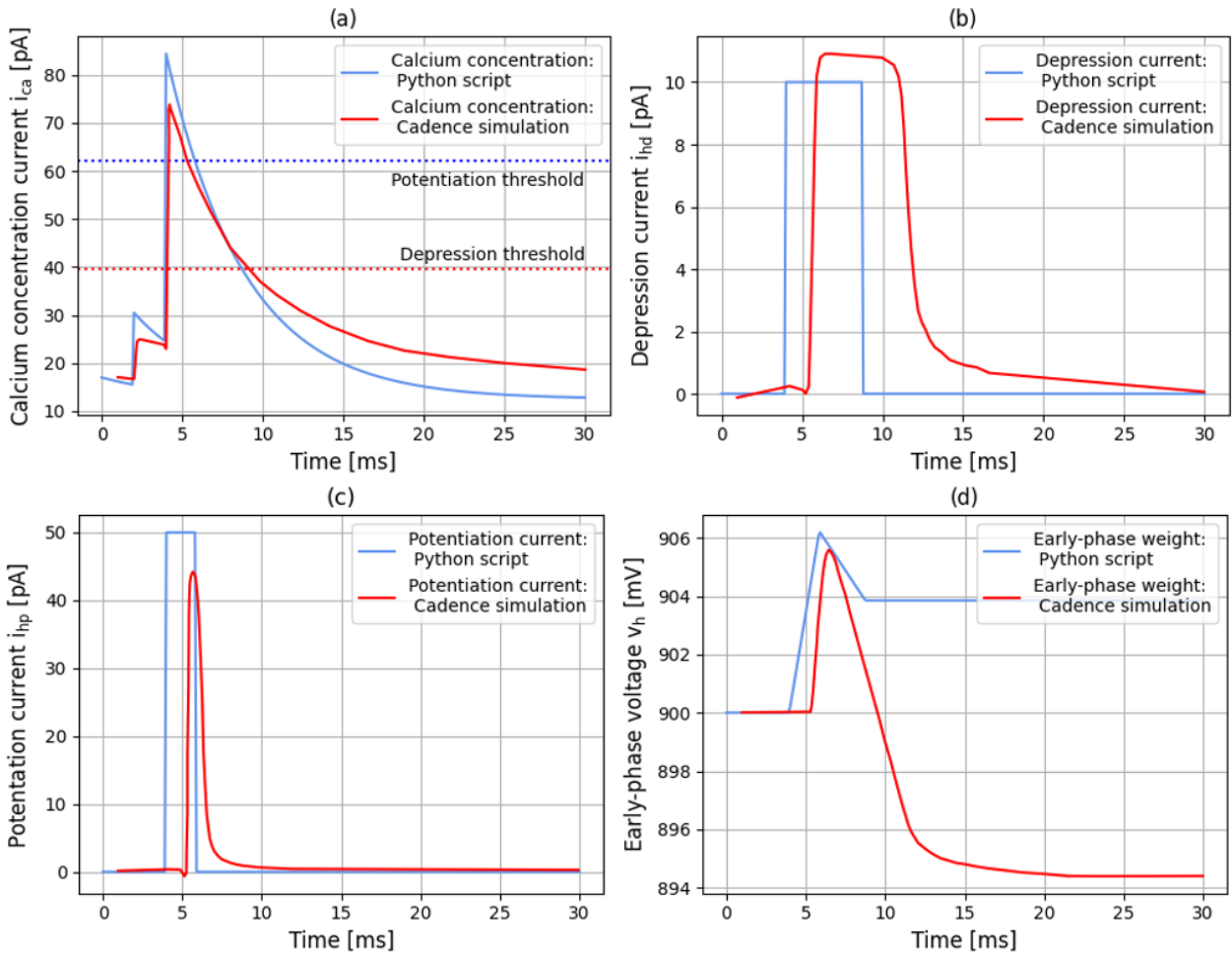


Figure 17: The influence of non-idealities on the behaviour of the synapse circuits. In red is the response of the synapse circuits simulated in Cadence Virtuoso, and in blue is the response of the Python script, using the same parameters and inputs as the Cadence simulation. (a) The response of the calcium concentration to a postsynaptic spike and a presynaptic spike, separated by 2 ms. (b) The depression current resulting from the change in the calcium concentration. (c) The potentiation current resulting from the change in the calcium concentration. (d) The early-phase response to the input, determined by the integration of the depression and potentiation currents. The results of the Cadence Virtuoso simulations are adapted from [12].

Although the general behaviours of both simulations, Python and Cadence, are similar, Figure 17 (d) shows different outcomes in the final EPW. This can be explained by the parasitic effects on the depression and potentiation currents. The calcium concentrations in both the Python script and Cadence simulation spend roughly equal amounts of time above the two thresholds, but despite this, the resulting depression and potentiation currents are not the same. The initiation of each of the two currents in the Cadence simulation exhibits a delay with regards to the calcium concentration crossing their respective thresholds, delaying the changes to the EPW with respect to the Python model. The currents also tail off gradually - owing to the characteristics of the ultra-low leakage blocks [12] used in the early-phase circuitry - rather than the instant drop the circuit logic suggests, extending the time that potentiation and depression are active. However, neither of these observations are sufficient in explaining the far steeper slopes, nor the dramatic depression, of the EPW observed in Figure 17 (d). This hints at the presence of other non-idealities within the early-phase circuitry or variability within

the Cadence simulation.

A comprehensive fitting of parameters, combined with updates to the Python script implementing certain parastics such as the delays or current pulse tails, would be possible. It would improve the mapping of the Python script behaviour onto the actual behaviour of the CMOS synapse. However, a full fit achieving this was not performed. The reasons for this are twofold: the parameters used were adequate in producing a functional neural network, and secondly, although the circuits have been taped out and the circuits are being fabricated, a physical version does not yet exist. The calibration of the circuit-based Python code has been scheduled for when the CMOS circuits are available, making it possible to base this calibration on the experimental characterisation of the circuits. This way, the simulations produced by the Python code will account for the influence of all the potential non-idealities the circuits may be subjected to.

Finally, the functionality of the CMOS synapse on a network level is demonstrated using a limited number of samples in the training and testing datasets. This limit was imposed by computing power, with larger datasets exceeding the RAM available. Access to a GPU would be required for a larger scale test, which would substantiate the accuracy results obtained. Larger scale tests are also needed in performing tests on the CMOS synapse's behaviour in biologically plausible networks (which the two-layer feedforward network used was not, owing to its lack of key features such as true inhibitory neurons, background noise, axonal time delay and plausible probabilities for a connection existing between two neurons [11, 30, 33]). However this is outside of the scope of this work, and hence has been left for future research; the small sample sizes used were sufficient in demonstrating this works objective, proving the functionality of the STC circuitry.

## 5 Conclusion

This work produced a Python code replicating the behaviour of a CMOS implementation of a synapse performing the biologically inspired multi-timescale learning rule STC. The accuracy of this Python code as an emulation of the circuit behaviour was tested through comparisons of the Python code to circuit simulations, performed in Cadence Virtuoso, and to an additional Python script created based on the differential equations governing STC. Once sufficient accuracy was achieved, the circuit-based Python code was used to test the CMOS circuitry on a network level. A two-layer, feedforward neural network was constructed to perform this testing, and the results revealed functionality of the network in distinguishing between MNIST sample ones and zeroes on both the early- and late-phase timescales. This meets the objective of this work, which set out to demonstrate the operation of the CMOS synapse on a network level.

This work is a milestone in a much larger project, and therefore there is a broad scope for future research. A comprehensive fitting of the Python code onto the behaviour of the physical circuits will have to be performed once they are taped out, and then the code will be used to test the operation of the CMOS synapse in a wide variety of applications. Such research could involve: the testing of the CMOS circuitry in more biologically plausible neural networks, such as recursive networks; using the networks to perform tasks more suited to the multi-timescale nature of STC, such as in keyword spotting; and ultimately, trying to achieve the long-term goal of implementing the proposed CMOS synapse into real-life edge computing applications.



## References

- [1] Scott McKinney et al. “International evaluation of an AI system for breast cancer screening”. In: *Nature* 577 (Jan. 2020), pp. 89–94. DOI: 10.1038/s41586-019-1799-6.
- [2] Awni Hannun et al. “Cardiologist-level arrhythmia detection and classification in ambulatory electrocardiograms using a deep neural network”. In: *Nature Medicine* 25 (Jan. 2019). DOI: 10.1038/s41591-018-0268-3.
- [3] Yikai Yang et al. “A Multimodal AI System for Out-of-Distribution Generalization of Seizure Identification”. In: *IEEE Journal of Biomedical and Health Informatics* PP (Mar. 2022), pp. 1–1. DOI: 10.1109/JBHI.2022.3157877.
- [4] Yikai Yang et al. “Weak self-supervised learning for seizure forecasting: a feasibility study”. In: *Royal Society Open Science* 9 (Aug. 2022). DOI: 10.1098/rsos.220374.
- [5] Oriol Vinyals et al. “Grandmaster level in StarCraft II using multi-agent reinforcement learning”. In: *Nature* 575 (Nov. 2019). DOI: 10.1038/s41586-019-1724-z.
- [6] David Silver et al. “Mastering the game of Go with deep neural networks and tree search”. In: *Nature* 529 (Jan. 2016), pp. 484–489. DOI: 10.1038/nature16961.
- [7] Jason Eshraghian et al. “Training Spiking Neural Networks Using Lessons From Deep Learning”. In: *Proceedings of the IEEE* PP (Sept. 2023), pp. 1–39. DOI: 10.1109/JPROC.2023.3308088.
- [8] Yufei Guo, Xuhui Huang, and Zhe Ma. “Direct learning-based deep spiking neural networks: a review”. In: *Frontiers in Neuroscience* 17 (June 2023). DOI: 10.3389/fnins.2023.1209795.
- [9] Yao Man et al. “Spike-based dynamic computing with asynchronous sensing-computing neuromorphic chip”. In: *Nature Communications* 15 (May 2024). DOI: 10.1038/s41467-024-47811-6.
- [10] Mahyar Shahsavari et al. “Advancements in spiking neural network communication and synchronization techniques for event-driven neuromorphic systems”. In: *Array* 20 (Oct. 2023), p. 100323. DOI: 10.1016/j.array.2023.100323.
- [11] Jannik Luboeinski and Christian Tetzlaff. “Organization and Priming of Long-term Memory Representations with Two-phase Plasticity”. In: *Cognitive Computation* 15 (June 2022), pp. 1–20. DOI: 10.1007/s12559-022-10021-7.
- [12] Jorge Quijada Navarro. “CMOS circuit design of a multi-timescale learning rule for spiking neural networks”. MA thesis. Technische Universität Dresden, 2024.
- [13] Kai Malcom and Josue Casco-Rodriguez. *A Comprehensive Review of Spiking Neural Networks: Interpretation, Optimization, Efficiency, and Best Practices*. Mar. 2023.
- [14] Jim Hsu, Carol Nilsson, and Fernanda Laezza. “Role of the Axonal Initial Segment in Psychiatric Disorders: Function, Dysfunction, and Intervention”. In: *Frontiers in Psychiatry* 5 (Aug. 2014), p. 109. DOI: 10.3389/fpsy.2014.00109.
- [15] Xiangwen Wang, Xianghong Lin, and Xiaochao Dang. “Supervised learning in spiking neural networks: A review of algorithms and evaluations”. In: *Neural Networks* 125 (May 2020), pp. 258–280. DOI: 10.1016/j.neunet.2020.02.011.
- [16] Atrayee Chatterjee and Souvik Paul. “An approach of curing Depression by Artificial Neural Networks(ANN) Approach with 5 Input Node Reviewing 3 Input Node”. In: *IJCSET* 6 (Dec. 2015), pp. 655–663.

- [17] Image courtesy of Tim Taylor.
- [18] Jia-Qin Yang et al. “Neuromorphic Engineering: From Biological to Spike-Based Hardware Nervous Systems”. In: *Advanced Materials* 32 (Nov. 2020), p. 2003610. DOI: 10.1002/adma.202003610.
- [19] Wulfram Gerstner and Kistler M. Werner. *Spiking Neuron Models: Single Neurons, Populations, Plasticity*. Aug. 2002. DOI: 10.1017/CBO9780511815706.
- [20] Federico Paredes-Vallés, Kirk Scheper, and Guido Croon. *Unsupervised Learning of a Hierarchical Spiking Neural Network for Optical Flow Estimation: From Events to Global Motion Perception*. Mar. 2019.
- [21] Alex Prodan and Richard Morris. “Synaptic Tagging and Capture: Functional Implications and Molecular Mechanisms”. In: Apr. 2024, pp. 1–41. ISBN: 978-3-031-54863-5. DOI: 10.1007/978-3-031-54864-2\_1.
- [22] Raheel Khan, Don Kulasiri, and Sandhya Samarasinghe. “A multifarious exploration of Synaptic Tagging and Capture hypothesis in synaptic plasticity: development of an integrated mathematical model and computational experiments”. In: *Journal of Theoretical Biology* 556 (Oct. 2022), p. 111326. DOI: 10.1016/j.jtbi.2022.111326.
- [23] Jannik Luboeinski and Christian Tetzlaff. “Memory consolidation and improvement by synaptic tagging and capture in recurrent neural networks”. In: *Communications Biology* 4 (Mar. 2021). DOI: 10.1038/s42003-021-01778-y.
- [24] Chiara Bartolozzi, Srinjoy Mitra, and Giacomo Indiveri. “An ultra low power current-mode filter for neuromorphic systems and biomedical signal processing”. In: Nov. 2006, pp. 130–133. ISBN: 978-1-4244-0436-0. DOI: 10.1109/BIOCAS.2006.4600325.
- [25] R. Edwards and Gert Cauwenberghs. “Synthesis of Log-Domain Filters from First-Order Building Blocks”. In: *Analog Integrated Circuits and Signal Processing* 22 (Mar. 2000), pp. 177–186. DOI: 10.1023/A:1008373826094.
- [26] John Lazzaro et al. “Winner-Take-All Networks of O(N) Complexity”. In: *Neural Information Processing Systems*. 1988. URL: <https://api.semanticscholar.org/CorpusID:1248336>.
- [27] Giacomo Indiveri. “A Current-Mode Hysteretic Winner-take-all Network, with Excitatory and Inhibitory Coupling”. In: *Analog Integr. Circuits Signal Process* 28 (Sept. 2001). DOI: 10.1023/A:1011208127849.
- [28] Shiva Subbulakshmi Radhakrishnan et al. “A biomimetic neural encoder for spiking neural network”. In: *Nature Communications* 12 (Apr. 2021). DOI: 10.1038/s41467-021-22332-8.
- [29] Soha Boroojerdi and George Rudolph. “Handwritten Multi-Digit Recognition With Machine Learning”. In: *2022 Intermountain Engineering, Technology and Computing (IETC)*. 2022, pp. 1–6. DOI: 10.1109/IETC54973.2022.9796722.
- [30] Peter Diehl and Matthew Cook. “Unsupervised learning of digit recognition using spike-timing-dependent plasticity”. In: *Frontiers in Computational Neuroscience* 9 (2015). ISSN: 1662-5188. DOI: 10.3389/fncom.2015.00099. URL: <https://www.frontiersin.org/articles/10.3389/fncom.2015.00099>.
- [31] Tobi Delbruck. “‘Bump’ circuits for computing similarity and dissimilarity of analog voltages”. In: *IJCNN-91-Seattle International Joint Conference on Neural Networks* i (1991), 475–479 vol.1. URL: <https://api.semanticscholar.org/CorpusID:16870681>.

- 
- [32] Sherin A. Thomas et al. “Analysis of Parasitics on CMOS based Memristor Crossbar Array for Neuromorphic Systems”. In: *2021 IEEE International Midwest Symposium on Circuits and Systems (MWSCAS)*. 2021, pp. 309–312. DOI: 10.1109/MWSCAS47672.2021.9531867.
  - [33] Yoshua Bengio et al. “Towards Biologically Plausible Deep Learning”. In: *CoRR* abs/1502.04156 (2015). arXiv: 1502.04156. URL: <http://arxiv.org/abs/1502.04156>.

## Appendices

### Appendix A

The complete code used to train and test the SNN implementing the CMOS synapse. A link to the digital version of the code is provided here:

<https://github.com/MANicholson/Modelling-and-Simulation-of-a-CMOS-Synapse-Implementing-Two-phase-Plasticity.git>

Complete code:

```

1  # Installs -----
2
3  !pip install snntorch
4  !pip install equinox
5
6  # Imports -----
7
8  import jax
9  import random
10 import jax.numpy as jnp
11 import numpy as np
12 import matplotlib.pyplot as plt
13 import equinox as eqx
14 import snntorch as snn
15 import torch
16 import numpy as np
17 from snntorch import spikegen
18 import pandas as pd
19
20 # Importing data -----
21 # Mounting drive
22
23 from google.colab import drive
24 drive.mount('/content/drive')
25
26 # Importing the data from drive
27
28 arr_full_path = '/content/drive/ ... '
29 df = pd.read_csv(arr_full_path)
30
31 arr_test_path = '/content/drive/ ... '
32 df_test = pd.read_csv(arr_test_path)
33
34
35 # Rate encoding of data -----
36
37 # Parameters required to produce spike input
38
39 spike_length = 150 # Length of time (in ms) each sample is presented to the network
40 gap_length = 200 # Length of time (in ms) between training samples
41 Number_synapses = 28*28
42 dt = 0.001 # Time step
43 max_spiking_frequency = 40 # Maximum spiking frequency in Hz
44
45 # Code to transform datasets into input spike arrays that will be fed to the
46 # neural network.
47
48 def generate_input_spikes(df, spike_length, dt, gap_length, number_synapses):
49     def generate_spike_train(value, length, dt):
50         frequency = (value / 255) * max_spiking_frequency
51         num_spikes = int(frequency * length * dt)
52         spike_train = np.zeros(length)
53
54         if num_spikes > 0:
55             if num_spikes >= length:

```

```

56         spike_train[:] = 1
57     else:
58         interval = length // num_spikes
59         for i in range(num_spikes):
60             spike_train[i * interval] = 1
61
62     return spike_train
63
64 def column_to_spike_array(column):
65     spike_array = []
66     for value in column:
67         spike_train = generate_spike_train(value, spike_length, dt)
68         spike_array.append(spike_train)
69         spike_array.append(np.zeros(gap_length))
70     return np.concatenate(spike_array)
71
72 input_spikes = []
73 for column in df.columns[1:]:
74     spike_array = jnp.array(column_to_spike_array(df[column]))
75     input_spikes.append(spike_array)
76
77 input_spikes = jnp.array(input_spikes)
78 input_spikes = input_spikes.reshape(number_synapses, 1, input_spikes.shape[1])
79
80 print("Output array shape:", input_spikes.shape)
81 return input_spikes
82
83 # Producing the training input
84
85 INPUT_SPIKES = generate_input_spikes(df, spike_length, dt, gap_length, Number_synapses)
86
87 # Producing the test input
88
89 INPUT_SPIKES_TEST = generate_input_spikes(df_test, spike_length, dt, gap_length, Number_synapses)
90
91 # Creating the stimulus input -----
92
93 # Parameters required to produce spike input
94
95 stimulus_magnitude = 1e-9 # Magnitude of stimulus current (in A)
96 number_secondary_neurons = 2 # Number of second layer neurons
97
98 def create_input_stimuli(df, spike_length, gap_length, stimulus_magnitude,
99                          number_secondary_neurons):
100     def create_input_stimulus(df, desired_value, stimulus_magnitude):
101         result_array = []
102         for value in df.iloc[:, 0]: # Iterate through the first column
103             if value == desired_value:
104                 result_array.extend([stimulus_magnitude] * spike_length)
105                 result_array.extend([0] * gap_length)
106             else:
107                 result_array.extend([-stimulus_magnitude] * spike_length)
108                 result_array.extend([0] * gap_length)
109         return np.array(result_array)
110
111     stimuli = []
112     for i in range(number_secondary_neurons):
113         stim = jnp.array([create_input_stimulus(df, i, stimulus_magnitude)])
114         stimuli.append(stim)
115
116     return stimuli
117
118 # Producing the stimulus input
119 stimuli = create_input_stimuli(df, spike_length, gap_length, stimulus_magnitude,
120                               number_secondary_neurons)
121
122 # Base code for the neural network -----
123
124 #
125
126 class many_synapse(eqX.Module):

```

```

127 tau_DPI: float
128 dt: float
129 delta_capre: float
130 delta_capost: float
131 I_TH: float
132 I_INDC: float
133 I_TAU: float
134 ica_0: float
135 C: float
136 v_h0: float
137 I_THPOT: float
138 I_THDEP: float
139 I_TAILP: float
140 I_TAILP_low: float
141 I_TAILD: float
142 I_TAILD_low: float
143 i_hrn: float
144 i_hrp: float
145 v_h0: float
146 V_DD: float
147 tau_z_c: float
148 z_max: float
149 z_min: float
150 theta_tag_c: float
151 alpha: float
152 theta_pro_circuit: float
153 z_0: float
154 beta: float
155 reset_voltage: float
156 V_rev: float
157 V_spike_threshold: float
158 tau_m: float
159 R_m: float
160 refractory_period: float
161 h_0: float = 0.0
162
163 def __call__(self, t_spike_pre_array, I_stim):
164     num_input_neurons = t_spike_pre_array.shape[0]
165
166     # Initial states
167     i_ca = jnp.zeros((num_input_neurons, 1)) + self.ica_0
168     v_h = jnp.zeros((num_input_neurons, 1)) + self.v_h0
169     z_ji = jnp.zeros((num_input_neurons, 1)) + self.z_0
170     w_ji = jnp.zeros((num_input_neurons, 1)) + self.beta * self.v_h0 + self.beta * self.v_h0 * self.z_0
171     V_i = jnp.zeros((1,)) + self.V_rev
172     p_i = jnp.zeros((num_input_neurons, 1))
173     t_spike_post = 0.0 # Initialize t_spike_post to 0
174     refractory_timer = jnp.zeros((1,))
175
176     # Lists to store the results
177     V_i_list = []
178     t_spike_post_list = []
179
180     def step(carry, input_):
181         t_spike_post, i_ca, v_h, z_ji, p_i, w_ji, V_i, refractory_timer = carry
182         t_spike_pre, I_stim = input_
183
184         # Code for the neurons in the second layer:.....
185
186         in_refractory = jnp.squeeze(refractory_timer > 0)
187         V_i = jax.lax.cond(in_refractory, lambda _: jnp.array([self.reset_voltage]), lambda _: V_i, operand=None)
188
189         inhibition_condition = jnp.squeeze(jnp.sum(I_stim) < 0)
190
191
192         reversal_term = (1 / self.tau_m) * (-V_i + self.V_rev)
193         pre_spike_contribution = (1 / self.tau_m) * jnp.sum(t_spike_pre * w_ji)
194         current_term = (1 / self.tau_m) * jnp.sum((self.R_m * I_stim))
195
196         spike_condition = jnp.squeeze(V_i > self.V_spike_threshold)
197

```

```

198     V_i_new = jax.lax.cond(spike_condition, lambda _:
199                             jnp.array([self.reset_voltage]),
200                             lambda _: V_i + (reversal_term + current_term)
201                             * self.dt + pre_spike_contribution, operand=None)
202     # For inhibition
203     V_i_new = jax.lax.cond(inhibition_condition, lambda _:
204                             jnp.array([self.reset_voltage]),
205                             lambda _: V_i + (reversal_term + current_term)
206                             * self.dt + pre_spike_contribution, operand=None)
207
208     # Update t_spike_post based on spike condition
209     t_spike_post_new = jax.lax.cond(spike_condition, lambda _: 1.0,
210                                     lambda _: 0.0, operand=None)
211     t_spike_post_list.append(t_spike_post_new)
212
213     # To enforce the refractory period
214     refractory_timer_new = jax.lax.cond(spike_condition, lambda _:
215                                         jnp.array([self.refractory_period]),
216                                         lambda _:
217                                             jax.numpy.maximum(refractory_timer - self.dt, 0),
218                                         operand=None)
219
220     # Calcium part -----
221     dica_dt = (1 / self.tau_DPI) * (-i_ca + self.I_TH * self.I_INDC / self.I_TAU)
222     ica_pre_increase = t_spike_pre * self.delta_capre
223     ica_post_increase = t_spike_post_new * self.delta_capost
224     i_ca_new = i_ca + dica_dt * self.dt + ica_pre_increase.T + ica_post_increase
225
226
227     # Early-phase part -----
228     recovery_condition = jnp.squeeze(v_h > self.v_h0)
229     potentiation_condition = jnp.squeeze(i_ca_new > self.I_THPOT)
230     depression_condition = jnp.squeeze(i_ca_new > self.I_THDEP)
231
232     i_recovery = jnp.array([jnp.where(recovery_condition, - self.i_hrn, self.i_hrp)])
233
234     i_potentiation = jnp.array([jnp.where(potentiation_condition, self.I_TAILP, self.I_TAILP_low)])
235
236     i_depression = jnp.array([jnp.where(depression_condition, - self.I_TAILD, self.I_TAILD_low)])
237
238     v_h_new = v_h + (1 / self.C) * (i_recovery.T + i_potentiation.T + i_depression.T) * self.dt
239
240     # Ensure v_h_new is not less than 0
241     v_h_new = jnp.maximum(v_h_new, 0)
242
243     # Late-phase part -----
244     epsilon_hi = jnp.abs(v_h_new - self.v_h0)
245     condition = jnp.array([jnp.squeeze(epsilon_hi > self.theta_pro_circuit)])
246
247     p_i = jnp.where(condition.T, self.alpha, p_i)
248     pot_term = p_i * (self.z_max - z_ji) * ((v_h_new - self.v_h0 - self.theta_tag_c) > 0)
249     dep_term = p_i * (z_ji - self.z_min) * ((self.v_h0 - v_h_new - self.theta_tag_c) > 0)
250     dz_dt = (1 / self.tau_z_c) * (pot_term - dep_term)
251     z_ji_new = z_ji + dz_dt * self.dt
252
253     # Ensure z_ji_new is not less than 0
254     z_ji_new = jnp.maximum(z_ji_new, 0)
255
256     # Total synaptic weight -----
257     w_ji_new = self.beta * v_h_new + self.beta * self.v_h0 * z_ji_new
258
259     V_i_list.append(V_i_new)
260
261     carry = (t_spike_post_new, i_ca_new, v_h_new, z_ji_new, p_i,
262             w_ji_new, V_i_new, refractory_timer_new)
263     return carry, (i_ca_new, v_h_new, z_ji_new, w_ji_new,
264                   V_i_new, t_spike_post_new)
265
266     carry = (t_spike_post, i_ca, v_h, z_ji, p_i, w_ji, V_i, refractory_timer)
267     _, (i_ca, v_h, z_ji, w_ji, V_i, t_spike_post) = jax.lax.scan(step, carry, (t_spike_pre_array.T, I_stim.T))
268

```

```

269         time_array = jnp.arange(len((i_ca.T)[0][0])) * self.dt
270
271         return i_ca.T, v_h.T, z_ji.T, w_ji.T, jnp.concatenate(V_i), t_spike_post, time_array
272
273     # Constants for differential code
274
275     # tc_delay = 0.0188 # Delay of postsynaptic calcium influx after presynaptic spike [s]
276     c_pre = 0.6 # Presynaptic calcium contribution [in vivo adjusted]
277     c_post = 0.1655 # Postsynaptic calcium contribution [in vivo adjusted]
278     tau_c = 0.0488 # Calcium time constant [s]
279     tau_h = 688.4 # ALTERED FROM 688.4 # Early-phase time constant [s]
280     tau_p = 60*60 # Protein time constant [s]
281     tau_z = 60*60 # Late-phase time constant [s]
282     # nu_th = 40 # Firing rate threshold for LTP induction [Hz]
283     gamma_p = 1645.6 # ALTERED FROM 1645.6 # Potentiation rate
284     gamma_d = 313.1 # ALTERED FROM 313.1 # Depression rate
285     theta_p = 0.003 # ALTERED FROM 3 # Calcium threshold for potentiation
286     theta_d = 0.002 # ALTERED FROM 1.2 # Calcium threshold for depression
287     # sigma_pl = 2.90436 * 10**(-3) # Standard deviation for plasticity fluctuations [V]
288     alpha = 1.0 # Protein synthesis rate
289     theta_pro = 0.003 # 2.10037 * 10**(-3) # Protein synthesis threshold [V]
290     theta_tag = 0.840149 * 10**(-3) # Tagging threshold [V]
291     h_0 = 4.20075 * 10**(-3) # Median initial excitatory excitatory coupling strength [V]
292     h_init = h_0
293     z_0 = 0.01
294     # Combining [12] and [11]
295
296     h_max = 10 * 10**(-3) # The maximum value of the early-phase variable [V]
297     z_max = 1 # The minimum value of the late-phase variable
298     z_min = - 0.5 # The maximum value of the late-phase variable
299
300     beta = 4.6675*10**(-3)
301
302     # Circuit-based code constants
303
304     # Calcium:
305     I_INDC = 25 * 10**(-12)
306     i_pre = 800 * 10**(-12)
307     i_post = 200 * 10**(-12)
308     tau_DPI = 0.00488
309     I_TH = 10 * 10**(-12)
310     I_TAU = 20 * 10**(-12)
311     ica_0 = 17 * 10**(-12)
312     delta_capre = 15 * 10**(-12)
313     delta_capost = 15 * 10**(-12)
314
315
316     # Early-phase:
317     tau_h_c = 68.84 # [s]
318     C = 1.2215 * 10**(-12)
319     v_H0 = 0.9
320     I_THPOT = 30 * 10**(-12)
321     I_THDEP = 25* 10**(-12)
322     I_TAILP = 50 * 10**(-12)
323     I_TAILP_low = 1.2 * 10**(-15)
324     I_TAILD = 10 * 10**(-12)
325     I_TAILD_low = 1.2 * 10**(-15)
326     i_hrp = 2.5 * 10**(-15)
327     i_hrn = 80 * 10**(-15)
328     v_h0 = 900 * 10**(-3)
329     V_DD = 1.8
330     z_0 = 0.0
331     # Late phase:
332     theta_tag_c = 0.0151226
333     theta_pro_circuit = 0.01
334     tau_z_c = 11.25
335     tau_p_c = 360
336
337     # Neuron constants
338
339     tau_m = 0.01

```



```

340 V_rev = -0.065 #
341 R_m = 10e6
342 reset_voltage = -0.07
343 V_spike_threshold = 70
344 refractory_period = 0.0001
345 dt = 0.001
346
347 # Training the network -----
348
349 manySynapse = many_synapse(
350     tau_DPI, dt, delta_capre, delta_capost, I_TH, I_INDC, I_TAU, ica_0,
351     C, v_H0, I_THPOT, I_THDEP, I_TAILP, I_TAILP_low, I_TAILD, I_TAILD_low, i_hrn, i_hrp,
352     v_h0, V_DD, tau_z_c, z_max, z_min, theta_tag_c, alpha, theta_pro_circuit,
353     z_0, beta, reset_voltage, V_rev, V_spike_threshold, tau_m, R_m, refractory_period
354 )
355
356 results = []
357
358 # Creating arrays with the final weights and plotting synaptic weights
359
360 for i, stim in enumerate(stimuli):
361     results.append(manySynapse(INPUT_SPIKES, stim))
362
363 final_weights = []
364 for i in range(number_secondary_neurons):
365     w_ji = results[i][3] # Assuming w_ji is the 4th returned value
366     final_values = w_ji[-1, :, -1]
367     final_weights.append(final_values)
368
369 print(len(final_weights))
370
371 # Plotting heatmaps
372 fig, axs = plt.subplots(1, number_secondary_neurons, figsize=(15, 5))
373
374 for i, weights in enumerate(final_weights):
375     square_grid = weights.reshape((28, 28))
376
377     im = axs[i].imshow(square_grid, cmap='hot', interpolation='nearest')
378     axs[i].set_title(f'Synaptic weights connecting output neuron \'{i}\''nto input
379                     neurons in first layer')
380
381     plt.colorbar(im)
382     axs[i].set_ylabel('Synaptic weight [mV]', fontsize = 12)
383     axs[i].set_xlabel('Synaptic index - horizontal', fontsize = 12)
384     axs[0].set_ylabel('Synaptic index - vertical', fontsize = 12)
385
386
387 plt.show()
388 plt.tight_layout()
389
390 # Testing the network -----
391
392 tau_m = 0.01
393 V_rev = -0.065 #
394 R_m = 10e6
395 reset_voltage = -0.07
396 V_spike_threshold = 70
397 refractory_period = 0.0001
398 dt = 0.001
399
400 class test_Network(eqx.Module):
401     tau_DPI: float
402     dt: float
403     delta_capre: float
404     delta_capost: float
405     I_TH: float
406     I_INDC: float
407     I_TAU: float
408     ica_0: float
409     C: float
410     v_H0: float

```

```

411 I_THPOT: float
412 I_THDEP: float
413 I_TAILP: float
414 I_TAILP_low: float
415 I_TAILD: float
416 I_TAILD_low: float
417 i_hrn: float
418 i_hrp: float
419 v_h0: float
420 V_DD: float
421 tau_z_c: float
422 z_max: float
423 z_min: float
424 theta_tag_c: float
425 alpha: float
426 theta_pro_circuit: float
427 z_0: float
428 beta: float
429 reset_voltage: float
430 V_rev: float
431 V_spike_threshold: float
432 tau_m: float
433 R_m: float
434 refractory_period: float
435 h_0: float = 0.0
436
437 def __call__(self, t_spike_pre_array, w_ji):
438     num_input_neurons = t_spike_pre_array.shape[0]
439
440     # Initial states
441     V_i = jnp.zeros((1,)) + self.V_rev
442     t_spike_post = 0.0 # Initialize t_spike_post to 0
443     refractory_timer = jnp.zeros((1,))
444     W_ji = w_ji.T
445
446     # Lists to store the results
447     V_i_list = []
448     t_spike_post_list = []
449
450     def step(carry, input_):
451         t_spike_post, V_i, refractory_timer, w_ji = carry
452         t_spike_pre = input_
453
454         # Code for the neurons in the second layer:.....
455
456         in_refractory = jnp.squeeze(refractory_timer > 0)
457         V_i = jax.lax.cond(in_refractory, lambda _: jnp.array([self.reset_voltage]),
458                          lambda _: V_i, operand=None)
459
460         reversal_term = (1 / self.tau_m) * (-V_i + self.V_rev)
461         pre_spike_contribution = (1 / self.tau_m) * jnp.sum(t_spike_pre * W_ji)
462         # print(t_spike_pre)
463         # print(w_ji)
464         # print(jnp.sum(t_spike_pre * W_ji))
465
466         spike_condition = jnp.squeeze(V_i > self.V_spike_threshold)
467
468         V_i_new = jax.lax.cond(spike_condition, lambda _: jnp.array([self.reset_voltage]),
469                              lambda _:
470                              V_i + (reversal_term) * self.dt + pre_spike_contribution,
471                              operand=None)
472
473         # Update t_spike_post based on spike condition
474         t_spike_post_new = jax.lax.cond(spike_condition, lambda _: 1.0, lambda _: 0.0,
475                                         operand=None)
476         t_spike_post_list.append(t_spike_post_new)
477
478         refractory_timer_new = jax.lax.cond(spike_condition, lambda _:
479                                             jnp.array([self.refractory_period]),
480                                             lambda _:
481                                             jax.numpy.maximum(refractory_timer - self.dt, 0),

```

```

482                                     operand=None)
483
484         V_i_list.append(V_i_new)
485
486         carry = (t_spike_post_new, V_i_new, refractory_timer_new, w_ji)
487
488         return carry, (V_i_new, t_spike_post_new)
489
490     carry = (t_spike_post, V_i, refractory_timer, w_ji)
491     _, (V_i, t_spike_post) = jax.lax.scan(step, carry, (t_spike_pre_array.T))
492
493     time_array = jnp.arange(len((t_spike_post))) * self.dt
494
495     return V_i, t_spike_post, time_array
496
497 # Running the test
498
499 network_test = test_Network(
500     tau_DPI, dt, delta_capre, delta_capost, I_TH, I_INDC, I_TAU, ica_0,
501     C, v_H0, I_THPOT, I_THDEP, I_TAILP, I_TAILP_low, I_TAILD, I_TAILD_low, i_hrn, i_hrp,
502     v_h0, V_DD, tau_z_c, z_max, z_min, theta_tag_c, alpha, theta_pro_circuit, z_0, beta,
503     reset_voltage, V_rev, V_spike_threshold, tau_m, R_m, refractory_period
504 )
505
506 number_secondary_neurons = len(final_weights)
507 number_test_samples = len(df_test)
508 print("number test samples:", number_test_samples)
509
510 # Initialize results_matrix with appropriate dimensions
511 results_matrix = np.zeros((number_secondary_neurons, number_test_samples))
512
513 # Run network_test for each final weight
514 for neuron_idx, final_weight in enumerate(final_weights):
515     V_i, t_spike_post, _ = network_test(INPUT_SPIKES_TEST, final_weight/4)
516
517     # Divide t_spike_post into subarrays
518     subarray_length = len(t_spike_post) // number_test_samples
519     t_spike_post_subarrays = np.array_split(t_spike_post, number_test_samples)
520
521     for row_idx, subarray in enumerate(t_spike_post_subarrays):
522         results_matrix[neuron_idx, row_idx] = jnp.sum(subarray)
523
524 # Find the secondary neuron that fired the most for each row
525 most_firing_neurons = np.argmax(results_matrix, axis=0)
526
527 print(len(most_firing_neurons)) # Verify length of most_firing_neurons
528
529 # Compare with the actual labels
530 correct_predictions = 0
531 for row_idx, row in df_test.iterrows():
532     true_label = row[0]
533     predicted_label = most_firing_neurons[row_idx]
534     if predicted_label == true_label:
535         correct_predictions += 1
536
537 print(most_firing_neurons) # Print most_firing_neurons for debugging
538 print(correct_predictions) # Print correct_predictions for debugging
539
540 # Calculate and print accuracy
541 accuracy = correct_predictions / number_test_samples
542 print(f"Accuracy: {accuracy * 100:.2f}%")
543
544

```

## Appendix B

The differential equation-based code used to train test whether the circuit-based code performed STC. A link to the digital version of the code is provided here:

<https://github.com/MANicholson/Modelling-and-Simulation-of-a-CMOS-Synapse-Implementing-Two-phase-Plasticity.git>

The code:

```

1  # Installs -----
2  pip install equinox
3
4  # Imports -----
5  import jax
6  import random
7  import jax.numpy as jnp
8  import matplotlib.pyplot as plt
9  import equinox as eqx
10
11 # Differential equations solved using the forward Euler method -----
12
13 class full_synapse_diff(eqx.Module):
14     # Calcium constants -----
15     c_pre: float
16     c_post: float
17     tau_c: float
18     dt: float
19     c_0: float
20     # Early-phase constants -----
21     tau_h: float
22     h_max: float
23     gamma_p: float
24     gamma_d: float
25     theta_p: float
26     theta_d: float
27     h_0: float
28     h_init: float
29     # Late-phase constants -----
30     tau_z: float
31     z_max: float
32     z_min: float
33     theta_tag: float
34     alpha: float
35     theta_pro: float
36     z_0: float
37
38     def __init__(self, c_pre, c_post, tau_c, dt, c_0, tau_h, h_max, gamma_p,
39                 gamma_d, theta_p, theta_d, h_0, h_init, tau_z, z_max, z_min,
40                 theta_tag, alpha, theta_pro, z_0):
41         # Calcium constants -----
42         self.c_pre = c_pre
43         self.c_post = c_post
44         self.tau_c = tau_c
45         self.dt = dt
46         self.c_0 = c_0
47         # Early-phase constants -----
48         self.tau_h = tau_h
49         self.h_max = h_max
50         self.gamma_p = gamma_p
51         self.gamma_d = gamma_d
52         self.theta_p = theta_p
53         self.theta_d = theta_d
54         self.h_0 = h_0
55         self.h_init = h_init
56         # Late-phase constants -----
57         self.tau_z = tau_z
58         self.z_max = z_max
59         self.z_min = z_min
60         self.theta_tag = theta_tag
61         self.alpha = alpha
62         self.theta_pro = theta_pro
63         self.z_0 = z_0
64
65     def __call__(self, input_):
66

```

```

67     # Calcium part -----
68     c_ji_0 = jnp.zeros((1,)) + self.c_0 # Initial state
69
70     def differential_eq_calcium(c_ji, input_):
71         t_spike_pre, t_spike_post = input_
72
73         dc_dt = -c_ji / self.tau_c
74         c_pre_increase = t_spike_pre * self.c_pre
75         c_post_increase = t_spike_post * self.c_post
76
77         c_ji_new = c_ji + dc_dt * self.dt + c_pre_increase + c_post_increase
78
79         return c_ji_new, c_ji_new
80
81     _, c_ji = jax.lax.scan(differential_eq_calcium, c_ji_0, input_)
82
83     time_array = jnp.arange(len(c_ji)) * self.dt
84
85     # Early-phase part -----
86     if self.h_init is None:
87         self.h_init = self.h_0
88
89     h_ji_0 = jnp.zeros((1,)) + self.h_init
90
91     def differential_eq_early_phase(h_ji, c_ji):
92         # Early-phase weight decay:
93         decay_term = (1 / self.tau_h) * 0.1 * (self.h_0 - h_ji)
94
95         # Early-phase LTP (potentiation occurs when the calcium concentration
96         # surpasses the specified threshold)
97         ltp_term = (1 / self.tau_h) * self.gamma_p * (self.h_max - h_ji) *
98                     (c_ji > self.theta_p)
99
100        # Early-phase LTD (depression occurs when the calcium concentration
101        # surpasses the specified threshold)
102        ltd_term = (1 / self.tau_h) * self.gamma_d * h_ji * (c_ji > self.theta_d)
103
104        # Combine terms
105        dh_dt = decay_term + ltp_term - ltd_term
106
107        # Update the early-phase variable using Euler's method
108        h_ji_new = h_ji + dh_dt * self.dt
109
110        return h_ji_new, h_ji_new
111
112    _, h_ji = jax.lax.scan(differential_eq_early_phase, h_ji_0, c_ji)
113
114    # Late-phase part -----
115    z_ji_0 = jnp.zeros((1,)) + self.z_0
116
117    # Set the protein availability to 0:
118    p_i = 0.0
119
120    def differential_eq_late_phase(carry, input_):
121        z_ji, p_i = carry
122        h_ji, c_ji = input_
123
124        # Early-phase change of neuron i
125        epsilon_hi = jnp.abs(h_ji - self.h_0)
126
127        # Check if the early-phase change is sufficient to trigger protein synthesis:
128        condition = jnp.squeeze(epsilon_hi > self.theta_pro)
129        p_i = jax.lax.cond(condition, lambda _: self.alpha, lambda _: p_i, operand=None)
130
131        # Calculate the change in late-phase variable based on the differential equation.
132
133        # Potentiation contribution
134        pot_term = p_i * (self.z_max - z_ji) * ((h_ji - self.h_0 - self.theta_tag) > 0)
135
136        # Depression contribution
137        dep_term = p_i * (z_ji - self.z_min) * ((self.h_0 - h_ji - self.theta_tag) > 0)

```

```

138
139     # Combine terms to get the total change
140     dz_dt = (1 / self.tau_z) * (pot_term - dep_term)
141
142     # Update late-phase variable using Euler's method
143     z_ji_new = z_ji + dz_dt * self.dt
144
145     return (z_ji_new, p_i), z_ji_new
146
147     carry = (z_ji_0, p_i)
148     inputs = (h_ji, c_ji)
149     _, z_ji = jax.lax.scan(differential_eq_late_phase, carry, inputs)
150
151     # Calculate the total synaptic weight -----
152
153     w_ji_0 = jnp.zeros((1,)) + h_ji_0 + h_ji_0 * z_ji_0
154
155
156     def total_synaptic_weight(w_ji, Inputs_):
157         h_ji, z_ji = Inputs_
158
159         w_ji_new = h_ji + h_ji_0 * z_ji
160
161         return w_ji_new, w_ji_new
162
163
164     Inputs_ = (h_ji, z_ji)
165     _, w_ji = jax.lax.scan(total_synaptic_weight, w_ji_0, Inputs_)
166
167     return c_ji, h_ji, z_ji, w_ji, time_array
168
169 # Testing -----
170
171 # Defining constants:
172
173 # tc_delay = 0.0188 # Delay of postsynaptic calcium influx after presynaptic spike [s]
174 c_pre = 0.6 # Presynaptic calcium contribution [in vivo adjusted]
175 c_post = 0.1655 # Postsynaptic calcium contribution [in vivo adjusted]
176 tau_c = 0.0488 # Calcium time constant [s]
177 tau_h = 688.4 # ALTERED FROM 688.4 # Early-phase time constant [s]
178 tau_p = 60*60 # Protein time constant [s]
179 tau_z = 60*60 # Late-phase time constant [s]
180 # nu_th = 40 # Firing rate threshold for LTP induction [Hz]
181 gamma_p = 1645.6 # ALTERED FROM 1645.6 # Potentiation rate
182 gamma_d = 313.1 # ALTERED FROM 313.1 # Depression rate
183 theta_p = 0.3 # ALTERED FROM 3 # Calcium threshold for potentiation
184 theta_d = 0.2 # ALTERED FROM 1.2 # Calcium threshold for depression
185 # sigma_pl = 2.90436 * 10**(-3) # Standard deviation for plasticity fluctuations [V]
186 alpha = 1.0 # Protein synthesis rate
187 theta_pro = 0.0023 # 2.10037 * 10**(-3) # Protein synthesis threshold [V]
188 theta_tag = 0.640149 * 10**(-4) # Tagging threshold [V]
189 h_0 = 4.20075 * 10**(-3) # Median initial excitatory*excitatory coupling strength [V]
190 h_init = h_0
191 z_0 = 0.1
192
193 # Constants required to combine results from following the logic of the circuits in
194 # "CMOS circuit design of a multi-timescale learning rule for spiking neural
195 # networks" by Jorge Navarro Quijada
196 # and the results obtained using the differential equations in
197 # https://doi.org/10.1007/s12559-022-10021-7
198
199 h_max = 10 * 10**(-3) # The maximum value of the early-phase variable [V]
200 z_max = 1 # The minimum value of the late-phase variable
201 z_min = - 0.5 # The maximum value of the late-phase variable
202
203 # beta = 4.6675*10**(-3)
204
205 # Creating test input:
206
207 import jax
208 import jax.numpy as jnp

```

[illegible]

---

```

280 synapseModel = full_synapse_diff(c_pre, c_post, tau_c, dt, 0, tau_h, h_max,
281                                 gamma_p, gamma_d, theta_p, theta_d, h_0, h_init,
282                                 tau_z, z_max, z_min, theta_tag, alpha, theta_pro, z_0)
283
284 c_ji_eqx, h_ji_eqx, z_ji_eqx, w_ji_eqx, t_eqx = synapseModel((jnp.array(t_spike_pre_new),
285                                                              jnp.array(t_spike_post_new)))

```

## Appendix C

The constants used in the creation of Figure 9. The first table presents the constants used in the circuit-based code, and the second table presents the constants used in the differential equation-based code.



Variable	Value	Unit	Description
I <sub>LINDC</sub>	$25 \times 10^{-12}$	A	The DC component of the tail current to stimulate the DPI.
$\tau_{DPI}$	0.00488	s	The time constant of the DPI.
I <sub>TH</sub>	$10 \times 10^{-12}$	A	The current to tune the gain of the DPI.
I <sub>TAU</sub>	$20 \times 10^{-12}$	A	The current to tune the time constant of the DPI.
delta_capre	$60 \times 10^{-12}$	A	The contribution of a presynaptic spike to the calcium concentration current.
delta_capost	$15 \times 10^{-12}$	A	The contribution of a postsynaptic spike to the calcium concentration current.
$\tau_{hc}$	68.84	s	The early-phase time constant.
C	$1.2215 \times 10^{-12}$	C	The capacitance of the capacitor.
v <sub>H0</sub>	0.9	V	The reference value of the EPW voltage.
I <sub>THPOT</sub>	$62 \times 10^{-12}$	A	The early-phase potentiation threshold for the calcium concentration.
I <sub>THDEP</sub>	$55 \times 10^{-12}$	A	The early-phase depression threshold for the calcium concentration.
I <sub>TAILP</sub>	$90 \times 10^{-12}$	A	The magnitude of the HIGH potentiation current.
I <sub>TAILP_low</sub>	$1.2 \times 10^{-15}$	A	The magnitude of the LOW potentiation current.
I <sub>TAILD</sub>	$10 \times 10^{-12}$	A	The magnitude of the HIGH depression current.
I <sub>TAILD_low</sub>	$0.8 \times 10^{-15}$	A	The magnitude of the LOW depression current.
i <sub>hrp</sub>	$2.5 \times 10^{-15}$	A	The magnitude of the potentiating-recovery current.
i <sub>hrn</sub>	$2.5 \times 10^{-15}$	A	The magnitude of the depressing-recovery current.
V <sub>DD</sub>	1.8	V	The maximum value of the EPW voltage.
theta_tag_c	0.0151226	A	The tagging threshold for a synaptic tag to be formed.
theta_pro_circuit	0.45	A	The protein capture threshold, for protein capture at a synapse to occur.
$\tau_{zc}$	360	s	The late-phase time constant.
beta	$4.6675 \times 10^{-3}$	n.a.	The factor used to match the outputs from portion of the code based on the circuits to the outputs based on the late-phase differential equation.

Table 1: Circuit-based Python script constants used in Figure 9. These are adapted from [12].

Variable	Value	Unit	Description
c_pre	0.6	mM	Presynaptic calcium contribution.
c_post	0.1655	mM	Postsynaptic calcium contribution.
$\tau_c$	0.0488	s	Calcium time constant.
$\tau_h$	688.4	s	Early-phase time constant.
$\tau_p$	3600	s	Protein time constant.
$\tau_z$	3600	s	Late-phase time constant.
gamma_p	1645.6	n.a.	Potential rate.
gamma_d	313.1	n.a.	Depression rate.
theta_p	0.3	mM	Calcium threshold for potentiation.
theta_d	0.2	mM	Calcium threshold for depression.
alpha	1.0	n.a.	Protein synthesis rate.
theta_pro	0.0023	V	Protein synthesis threshold.
theta_tag	$0.640149 \times 10^{-4}$	V	Tagging threshold.
h_0	$4.20075 \times 10^{-3}$	V	Median initial excitatory-excitatory coupling strength.
h_max	$10 \times 10^{-3}$	V	The maximum value of the early-phase variable.
z_max	1	V	The maximum value of the late-phase variable.
z_min	-0.5	V	The minimum value of the late-phase variable.

Table 2: Differential equation-based Python script constants used in Figure 9. These are adapted from [11].

**Appendix D**

The constants used in the training and testing of the neural network:

Variable	Value	Unit	Description
I_IND	$25 \times 10^{-12}$	A	The DC component of the tail current to stimulate the DPI.
$\tau_{DPI}$	0.00488	s	The time constant of the DPI.
I_TH	$10 \times 10^{-12}$	A	The current to tune the gain of the DPI.
I_TAU	$20 \times 10^{-12}$	A	The current to tune the time constant of the DPI.
ica_0	$17 \times 10^{-12}$	A	The initial calcium concentration current.
delta_capre	$15 \times 10^{-12}$	A	The contribution of a presynaptic spike to the calcium concentration current.
delta_capost	$15 \times 10^{-12}$	A	The contribution of a postsynaptic spike to the calcium concentration current.
$\tau_{h_c}$	68.84	s	The early-phase time constant.
C	$1.2215 \times 10^{-12}$	C	The capacitance of the capacitor.
v_H0	0.9	V	The reference value of the EPW voltage.
I_THPOT	$30 \times 10^{-12}$	A	The early-phase potentiation threshold for the calcium concentration.
I_THDEP	$25 \times 10^{-12}$	A	The early-phase depression threshold for the calcium concentration.
I_TAILP	$50 \times 10^{-12}$	A	The magnitude of the HIGH potentiation current.
I_TAILP_low	$1.2 \times 10^{-15}$	A	The magnitude of the LOW potentiation current.
I_TAILD	$10 \times 10^{-12}$	A	The magnitude of the HIGH depression current.
I_TAILD_low	$1.2 \times 10^{-15}$	A	The magnitude of the LOW depression current.
i_hrp	$2.5 \times 10^{-15}$	A	The magnitude of the potentiating-recovery current.
i_hrn	$80 \times 10^{-15}$	A	The magnitude of the depressing-recovery current.
v_h0	$900 \times 10^{-3}$	V	The initial value of the EPW voltage.
V_DD	1.8	V	The maximum value of the EPW voltage.
theta_tag_c	0.0151226	A	The tagging threshold for a synaptic tag to be formed.
theta_pro_circuit	0.02	A	The protein capture threshold, for protein capture at a synapse to occur.
$\tau_{z_c}$	360	s	The late-phase time constant.
z_0	0.0	V	The initial late-phase value.
$\tau_m$	0.01	s	The neuron membrane time constant.
V_rev	-0.065	V	The reversal voltage.
R_m	$10 \times 10^6$	$\Omega$	The resistance used in the LIF neuron.
reset_voltage	-0.07	V	The neuron reset voltage.
V_spike_threshold	70	V	The spiking threshold for the LIF neuron.
refractory_period	0.0001	s	The refractory period following a spike.

Table 3: List of constants used in the circuit-based Python code, adapted from [11] and [12].

## **Appendix E**

The following is a link to the code and input data used to produce all the relevant figures in the Results section:

<https://github.com/MANicholson/Figures-Modelling-and-Simulation-of-a-CMOS-Synapse-Implementing-Two-phase-Plasticity.git>